

# The caustic ring singularity

P. Sikivie

*Department of Physics, University of Florida, Gainesville, FL 32611*

(April 30, 2019)

## Abstract

I investigate the caustics produced by the fall of collisionless dark matter in and out of a galaxy in the limit of negligible velocity dispersion. The outer caustics are spherical shells enveloping the galaxy. The inner caustics are rings. These are located near where the particles with the most angular momentum are at their distance of closest approach to the galactic center. The surface of a caustic ring is a closed tube whose cross-section is a  $D_{-4}$  catastrophe. It has three cusps amongst which exists a discrete  $Z_3$  symmetry. A detailed analysis is given in the limit where the flow of particles is axially and reflection symmetric and where the transverse dimensions of the ring are small compared to the ring radius. Five parameters describe the caustic in that limit. The relations between these parameters and the initial velocity distribution of the particles are derived. The structure of the caustic ring is used to predict the shape of the bump produced in a galactic rotation curve by a caustic ring lying in the galactic plane.

## I. INTRODUCTION

There are compelling reasons to believe that the dark matter of the universe is constituted, at least in part, by non-baryonic collisionless particles with low primordial velocity dispersion [1]. Such particles are called cold dark matter. The leading candidates are axions and weakly interacting massive particles (WIMPs). Before the onset of galaxy formation but after the time  $t_{eq}$  of equality between matter and radiation, the velocity dispersion of the cold dark matter candidates is very small, of order  $\delta v_a(t) \sim 3 \cdot 10^{-17} \left(\frac{10^{-5} eV}{m_a}\right) \left(\frac{t_0}{t}\right)^{2/3}$  for axions and  $\delta v_W(t) \sim 10^{-11} \left(\frac{GeV}{m_W}\right)^{1/2} \left(\frac{t_0}{t}\right)^{2/3}$  for WIMPs, where  $t_0$  is the present age of the universe and  $m_a$  and  $m_W$  are respectively the masses of the axion and the WIMP. The above estimates of the primordial velocity dispersions,  $\delta v_a$  and  $\delta v_W$ , are very crude but our point is only that in the context of this paper, and of galaxy formation in general,  $\delta v_a$  and  $\delta v_w$  are entirely negligible. Massive neutrinos, on the other hand, have primordial velocity dispersion  $\delta v_\nu(t) \simeq 5.3 \cdot 10^{-4} \left(\frac{eV}{m_\nu}\right) \left(\frac{t_0}{t}\right)^{2/3}$  which is comparable to the virial velocity in galaxies and is therefore non-negligible in the context of galaxy formation [2]. For this reason, massive neutrinos are called “hot dark matter”.

Before the onset of galaxy formation, the collisionless dark matter particles lie on a thin 3-dimensional (3D) sheet in 6D phase-space. The thickness of this sheet is the primordial velocity dispersion  $\delta v$ . If each of the aforementioned species of collisionless particles is present, the phase-space sheet has three layers, a very thin layer of axions, a medium layer of WIMPs and a thick layer of neutrinos. The phase-space sheet is located on the 3D hypersurface of points  $(\vec{r}, \vec{v})$  :  $\vec{v} = H(t)\vec{r} + \Delta\vec{v}(\vec{r}, t)$  where  $H(t) = \frac{2}{3t}$  is the Hubble expansion rate and  $\Delta\vec{v}(\vec{r}, t)$  is the peculiar velocity field. Fig. 1 shows a 2D section of 6D phase-space along the  $(z, \dot{z})$  plane. The wiggly line is the intersection of the 3D sheet on which the particles lie in phase-space with the plane of the figure. The thickness of the line is the velocity dispersion  $\delta v$ , whereas the amplitude of the wiggles in the line is the peculiar velocity  $\Delta v$ . If there were no peculiar velocities, the line would be straight since  $\dot{z} = H(t)z$  in that case.

The peculiar velocities are associated with density perturbations and grow by gravitational instability as  $\Delta v \sim t^{2/3}$ . On the other hand the primordial velocity dispersion decreases on average as  $\delta v \sim t^{-2/3}$ , consistently with Liouville’s theorem. When a large overdensity enters the non-linear regime, the particles in the vicinity of the overdensity fall back onto it. This implies that the phase-space sheet “winds up” in clockwise fashion wherever an overdensity grows in the non-linear regime. One such overdensity is shown in Fig. 1. Before density perturbations enter the non-linear regime, there is only one value of velocity, i.e. one single flow, at a typical location in physical space, because the phase-space sheet covers physical space only once. On the other hand, inside an overdensity in the non-linear regime, the phase-space sheet covers physical space multiple times implying that there are several, but always an odd number of, flows at such locations in physical space.

At the boundary between two regions one of which has  $n$  flows and the other  $n + 2$  flows, the physical space density is very large because the phase-space sheet has a fold there. At the fold, the phase-space sheet is tangent to velocity space and hence, in the limit of zero velocity dispersion ( $\delta v = 0$ ), the density diverges since it is the integral of the phase-space density over velocity space. The structure associated with such a phase-space fold is called a

'caustic'. It is easy to show (see section II) that, in the limit of zero velocity dispersion, the density diverges as  $d \sim \frac{1}{\sqrt{\sigma}}$  when the caustic is approached from the side with  $n + 2$  flows, where  $\sigma$  is the distance to the caustic. If the velocity dispersion is small but non-zero, the divergence is cut off so that the density is no longer infinite at the caustic but merely very large.

In discussing this type of phenomenon, it is useful to adopt a parametrization of the phase-space sheet in the limit of zero velocity dispersion, by giving each particle a 3-parameter label  $\vec{\alpha} = (\alpha_1, \alpha_2, \alpha_3)$ . The phase-space sheet location at time  $t$  is specified by the map  $\vec{\alpha} \rightarrow \vec{x}(\vec{\alpha}, t)$  where  $\vec{x}$  is the position in physical space of particle  $\vec{\alpha}$  at time  $t$ . The velocity of particle  $\vec{\alpha}$  is  $\vec{v} = \frac{\partial \vec{x}}{\partial t}(\vec{\alpha}, t)$ . The density diverges wherever the map  $\vec{\alpha} \rightarrow \vec{x}$  is singular, i.e. where the Jacobian  $D \equiv \det \left( \frac{\partial \vec{x}}{\partial \vec{\alpha}} \right)$  vanishes. Thus caustics are associated with zeros of  $D$ . Since  $D = 0$  is one condition on three parameters, caustics are generically two dimensional surfaces.

Y. Zel'dovich [3] emphasized the importance of caustics in large scale structure formation, suggesting the name "pancakes" for them. The reason why galaxies tend to lie on surfaces [4], such as "the Great Wall", is undoubtedly that the 3D sheet on which the dark matter particles and baryons lie in phase-space acquires folds on very large scales, producing caustics appropriately called "Zel'dovich pancakes".

S. Tremaine [5] recently used the techniques of Catastrophe Theory [6] to catalogue the caustics which may occur in observations of structure formation.

We saw above that where a localized overdensity is growing in the non-linear regime, the line which is at the intersection of the phase-space sheet with the  $(z, \dot{z})$  plane winds up in clockwise fashion. The onset of this process is illustrated in Fig. 1. Of course, the picture is qualitatively the same in the  $(x, \dot{x})$  and  $(y, \dot{y})$  planes. In this view, the process of galactic halo formation is the winding up of the phase-space sheet of collisionless dark matter particles. When the galactic center is approached from any direction, the local number of flows increases. First, there is one flow, then three flows, then five, seven... The number of flows at our location in the Milky Way galaxy has been estimated to be of order 100 [7]. The boundary between the region with one (three, five, ...) and the region with three (five, seven, ...) flows is the location of a caustic which is topologically a sphere surrounding the galaxy. When these caustic spheres are approached from the inside the density diverges as  $d \sim \frac{1}{\sqrt{\sigma}}$  in the zero velocity dispersion limit. I call these spheres "outer" caustics to distinguish them from the "inner" caustics which are the main topic of this paper.

To see inner caustics, let us first discuss the case where the overdensity is spherically symmetric and all the dark matter particles carry zero angular momentum with respect to the center. All particles move on radial orbits then. As a result the galactic center is a caustic point where the density associated with each flow in and out of the galaxy diverges as  $d \sim \frac{1}{r^{1/2}}$  in the limit of zero velocity dispersion, where  $r$  is the radial coordinate. We remarked earlier that a caustic is generically a surface. Thus we find a caustic *point* only because we are assuming spherical symmetry and purely radial orbits. If these assumptions are relaxed, the caustic at the galactic center will spread over some size  $a$ . The notion of caustic point is nonetheless useful provided  $a$  is small enough. Indeed, for  $r \gg a$  the density will still behave as  $d \sim \frac{1}{r^{1/2}}$  and the phase-space structure will be qualitatively the same as for  $a = 0$ .

The question arises what is the inner caustic in the absence of spherical symmetry and in the presence of angular momentum. I. Tkachev, Y. Wang and I found [8,9] that the

inner caustic is a ring, i.e. a closed line. The density diverges as  $d \sim \frac{1}{\sigma}$  in the zero velocity dispersion limit where  $\sigma$  is the distance to the line [9]. However, as remarked earlier, a caustic is generically a surface. So a caustic line must again be a special degenerate case. Indeed, we will see below that a caustic ring is more precisely a closed tube with a special structure. Nonetheless, when the transverse dimensions, called  $p$  and  $q$  below, are small compared to the radius of curvature  $a$  of the tube,  $d \sim \frac{1}{\sigma}$  for  $a \gg \sigma \gg p, q$ . Hence, it makes sense to think of the caustic ring first as a closed line and then, on closer inspection, as a closed tube.

The next question is what is the structure of the tube. We find below that its transverse cross-section is a closed line with three cusps, one of which points away from the galactic center (see Figs. 5 and 6). In the language of Catastrophe Theory such a singularity is called a  $D_{-4}$  catastrophe [6]. It has a triality (i.e. a  $Z_3$  invariance) which is reminiscent of the triality of the Lie group  $D_4$ , also called  $SO(8)$ .

The existence of caustic rings of dark matter results from only two assumptions (see section III for a derivation):

1. the existence of collisionless dark matter
2. that the velocity dispersion of the infalling dark matter is much less, by a factor ten say, than the rotation velocity of the galaxy.

Only the second assumption requires elaboration. We noted earlier that velocity dispersion smoothes out caustics. The question is when is the velocity dispersion so large as to smooth caustic rings over distance scales of order the ring radius  $a$ , thus making the notion of caustic ring meaningless. In ref. [9] this critical velocity dispersion was estimated to be  $30 \text{ km/s} = 10^{-4}$  for the caustic rings in our own galaxy, whose rotation velocity is  $220 \text{ km/s}$ .  $10^{-4}$  is much less than the *primordial* velocity dispersion  $\delta v$  of the cold dark matter candidates. However the velocity dispersion  $\Delta v$  associated with density perturbations also smoothes caustics in coarse grained observations. From the point of view of an observer with infinite resolution, the effect of  $\Delta v$  on a caustic surface is to make it bumpy. However, to an observer with poor spatial resolution, this is the same as smoothing the surface. So the question is whether the velocity dispersion  $\Delta v$  of cold dark matter particles associated with density perturbations falling onto our galaxy is less than  $30 \text{ km/s}$ . The answer is yes with very high probability since the infalling dark matter particles are not associated with any observed inhomogeneities, and the velocity dispersion of an inhomogeneity as large as the Large Magellanic Cloud is still only  $10 \text{ km/s}$ . The only way the velocity dispersion of the infalling dark matter particles could be as large as say  $20 \text{ km/s}$  is for these particles to be part of clumps whose mass/size ratio is 4 times larger than that of the Large Magellanic Cloud. But if that were the case, why did these clumps fail to become luminous?

I have interpreted [9] the appearance of bumps in the rotation curves of NGC3198 and of our own galaxy as due to caustic rings of dark matter. That interpretation makes use of an additional assumption, namely that the infall of dark matter particles is self-similar [10,11,8]. This additional assumption is not used in this paper. The goal is to clearly distinguish those conclusions which follow exclusively from the two assumptions listed above from those conclusions which require the extra assumption of self-similarity. We are however motivated by the possibility that caustic rings may be observed as bumps in rotation curves and we

derive the shape that such a bump should ideally have. Gravitational lensing by caustic rings [12] is another technique by which these structures may be observed.

One might ask whether caustic rings can be seen in N-body simulations of galaxy formation. Zel'dovich pancakes are seen [13]. However, caustic rings would require far greater resolution than presently available, at least in a 3D simulation of our own halo. Indeed, the largest ring in our galaxy has been estimated to have radius of order 40 kpc [9]. It occurs in a flow that extends to the Galaxy's current turnaround radius, of order 2 Mpc. To resolve this first ring, the spatial resolution would have to be of order 10 kpc or smaller. Hence a minimum of  $2 \cdot \frac{1}{(10\text{kpc})^3} \frac{4\pi}{3} (2\text{Mpc})^3 \simeq 7 \cdot 10^7$  particles would be required to see the caustic ring in a simulation of this one flow. However, the number of flows at 40 kpc in our halo is of order 10 [8]. So it appears that several times  $10^8$  particles are necessary in a 3D simulation of our halo. This is a strict minimum because it only addresses the kinematic requirement of resolving the halo in phase-space, assuming moreover that the particles are approximately uniformly distributed on the phase-space sheets. There is a further dynamical requirement that 2-body collisions do not artificially 'fuzz up' the phase-space sheets. Indeed 2-body collisions are entirely negligible in the flow of cold dark matter particles such as axions or WIMPs. As a result, Liouville's theorem is strictly obeyed. On the other hand, 2-body collisions are present in N-body simulations and thus Liouville's theorem is violated. As a result the velocity dispersion is artificially increased in the simulations. This may occur to such an extent that the caustics are washed away even if several  $10^8$  particles are used. The best bet to see a caustic ring would obviously be in a 2D simulation of an axially symmetric flow.

This paper is organized as follows. In section II, we give a general discussion of caustic surfaces and caustic lines. Caustic lines are a degenerate case whereas caustic surfaces are generic. We distinguish two types of caustic line which we call *attached* and *isolated*. The former are attached to caustic surfaces whereas the latter are not. Caustic rings are of the *isolated* type. In section III, we discuss the caustics associated with the infall of collisionless dark matter particles onto a galaxy. We focus most of our attention on the inner caustic rings. We show that the presence of these rings follows only from the two assumptions listed above. We find that the ring is a tube. Inside the tube are four flows whereas outside the tube are two flows. (In addition there is an odd number of flows which are not associated with the caustic ring.) In section IV, we give a detailed analysis of the caustic ring under the additional assumptions that the flow is axially and reflection symmetric and that the transverse dimensions of the ring,  $p$  and  $q$ , are small compared to the ring radius  $a$ . In section IVA, we show that under these assumptions the flow near the ring is described in terms of five parameters:  $a$ ,  $b$ ,  $\tau_0$ ,  $u$  and  $s$ . In section IVB, we relate these parameters to the velocity distribution of the infalling dark matter particles. In section IVC, we give a qualitative description of the flow of particles on distance scales of order the ring radius  $a$ . In section V, the results of section IV are used to derive the shape of the bump a caustic ring causes in a galactic rotation curve if the ring lies in the galactic plane and the rotation curve is measured in the galactic plane. Section VI summarizes the conclusions.

## II. CAUSTICS IN GENERAL

Consider a flow of collisionless particles with zero (or negligible) velocity dispersion. Being collisionless, the particles obey Liouville's theorem. Since they have negligible velocity dispersion, the particles lie on a time-dependent 3D sheet in 6D phase-space. The flow is completely specified by giving the spatial coordinates  $\vec{x}(\vec{\alpha}, t)$  of the particle labeled  $\vec{\alpha}$  at time  $t$ , for all  $\vec{\alpha}$  and  $t$ . The 3-parameter label  $\vec{\alpha}$  is chosen arbitrarily. Let  $\vec{\alpha}_j(\vec{x}, t)$ , with  $j = 1 \dots n$ , be the solutions of  $\vec{x} = \vec{x}(\vec{\alpha}, t)$ .  $n$  is the number of distinct flows at  $\vec{x}$  and  $t$ . The total number of particles is:

$$N = \int d^3\alpha \frac{d^3N}{d\alpha_1 d\alpha_2 d\alpha_3}(\vec{\alpha}) = \int d^3x \sum_{j=1}^n \frac{d^3N}{d\alpha_1 d\alpha_2 d\alpha_3}(\vec{\alpha}_j(\vec{x}, t)) \frac{1}{|\det\left(\frac{\partial\vec{x}}{\partial\vec{\alpha}}\right)|_{\vec{\alpha}_j(\vec{x}, t)}}. \quad (2.1)$$

The density of particles in physical space is thus:

$$d(\vec{x}, t) = \sum_{j=1}^n \frac{d^3N}{d\alpha_1 d\alpha_2 d\alpha_3}(\vec{\alpha}_j(\vec{x}, t)) \frac{1}{|D(\vec{\alpha}, t)|_{\vec{\alpha}_j(\vec{x}, t)}}, \quad (2.2)$$

where

$$D(\vec{\alpha}, t) \equiv \det\left(\frac{\partial\vec{x}}{\partial\vec{\alpha}}\right). \quad (2.3)$$

The formula for the density is, of course, reparametrization invariant. Caustics occur wherever  $D = 0$ , i.e. where the map  $\vec{\alpha} \rightarrow \vec{x}$  is singular. At the caustic the density diverges. The divergence is cut off if the velocity dispersion is finite.

Generically the zeros of  $D$  are simple, i.e. the matrix  $\frac{\partial\vec{x}}{\partial\vec{\alpha}}$  has a single vanishing eigenvalue. The condition that one eigenvalue vanishes imposes one constraint on the three parameters  $\vec{\alpha}$ . Hence a caustic is generically a 2D surface in physical space.

### A. Generic surface caustics

Consider a generic surface caustic at a fixed time  $t$ . We may reparametrize the flow near the caustic,  $\vec{\alpha} \rightarrow \vec{\beta} = \vec{\beta}(\vec{\alpha}, t)$ , such that the caustic surface is at  $\beta_3 = 0$ . Also, in a neighborhood of a point on the surface, choose Cartesian coordinates such that  $\hat{z}$  is perpendicular to the surface whereas  $\hat{x}$  and  $\hat{y}$  are parallel. We have then:

$$D = \frac{\partial z}{\partial\beta_3} \det\left(\frac{\partial(x, y)}{\partial(\beta_1, \beta_2)}\right) \quad (2.4)$$

near that point. The 2-dim. matrix  $\frac{\partial(x, y)}{\partial(\beta_1, \beta_2)}$  is non-singular. Since  $D = 0$  at  $\beta_3 = 0$ , we have

$$z = z_0 + B\beta_3^2 \quad (2.5)$$

for small  $\beta_3$ . We may orient the  $\hat{z}$ -axis in such a way that  $B > 0$ . Then

$$D = 2\sqrt{B(z - z_0)} \det\left(\frac{\partial(x, y)}{\partial(\beta_1, \beta_2)}\right) \quad \text{for } z > z_0. \quad (2.6)$$

Hence, near a caustic surface located at  $z = z_0$ , the density diverges as  $\frac{1}{\sqrt{z-z_0}}$  on one side of the surface.

Fig. 2a shows a 2D cut of phase-space along the  $(z, \dot{z})$  plane. The particles lie on a line which is at the intersection of the phase-space sheet with the  $(z, \dot{z})$  plane. The label  $\beta_3$  gives the position of the particles along the line. In the example of the figure, there are two caustic surfaces, one at  $z = z_1$  and the other at  $z = z_2$ . The two dimensions ( $x$  and  $y$ ) into which the caustic extends as a surface are not shown. The density  $d(z)$ , shown in Fig. 2b, diverges as  $\frac{1}{\sqrt{z-z_1}}$  for  $z \rightarrow z_1$  with  $z > z_1$  and as  $\frac{1}{\sqrt{z_2-z}}$  for  $z \rightarrow z_2$  with  $z < z_2$ . For  $z_1 < z < z_2$  there are three flows ( $n = 3$ ) whereas for  $z < z_1$  and  $z > z_2$  there is only one flow ( $n = 1$ ). The phase-space sheet “folds back” at  $z = z_1$  and  $z = z_2$ . That is why the map  $\beta \rightarrow z$  is singular at these locations.

## B. Line caustics

Next, consider places where  $D$  has a double zero, i.e. where  $\frac{\partial \vec{x}}{\partial \vec{\alpha}}$  has vanishing eigenvalues for two different eigenvectors. The condition that two eigenvalues vanish defines a line. This line is the location of a more singular kind of caustic which we call ‘line caustic’.

In a small neighborhood of a line caustic let us reparametrize the flow ( $\vec{\alpha} \rightarrow \vec{\beta}$ ) such that  $\beta_1 = \beta_2 = 0$  defines the line in the new coordinates. Also, choose Cartesian coordinates such that  $\hat{z}$  is parallel to the line and  $\hat{x}$  and  $\hat{y}$  are perpendicular to it. In this neighborhood we have:

$$D = \frac{\partial z}{\partial \beta_3} \det \left( \frac{\partial(x, y)}{\partial(\beta_1, \beta_2)} \right) \quad (2.7)$$

with  $\frac{\partial z}{\partial \beta_3} \neq 0$ . At  $\beta_1 = \beta_2 = 0$ , the matrix  $\frac{\partial(x, y)}{\partial(\beta_1, \beta_2)}$  vanishes since it is 2x2 and has vanishing eigenvalues for two different eigenvectors. Thus for small  $\beta_1$  and  $\beta_2$ ,

$$\begin{aligned} x &= x_0 + \frac{1}{2}X_{11}\beta_1^2 + X_{12}\beta_1\beta_2 + \frac{1}{2}X_{22}\beta_2^2 + 0(\beta^3) \\ y &= y_0 + \frac{1}{2}Y_{11}\beta_1^2 + Y_{12}\beta_1\beta_2 + \frac{1}{2}Y_{22}\beta_2^2 + 0(\beta^3) . \end{aligned} \quad (2.8)$$

Linear combinations  $x - x_0 + \gamma(y - y_0)$  are complete squares provided:

$$\gamma^2(Y_{11}Y_{22} - Y_{12}^2) + \gamma(Y_{11}X_{22} + X_{11}Y_{22} - 2X_{12}Y_{12}) + X_{11}X_{22} - X_{12}^2 = 0 , \quad (2.9)$$

which has two solutions:

$$\begin{aligned} \gamma_{\pm} &= \frac{1}{2(Y_{11}Y_{22} - Y_{12}^2)} \{ -Y_{11}X_{22} - X_{11}Y_{22} + 2X_{12}Y_{12} \\ &\pm [(Y_{11}X_{22} + X_{11}Y_{22} - 2X_{12}Y_{12})^2 - 4(Y_{11}Y_{22} - Y_{12}^2)(X_{11}X_{22} - X_{12}^2)]^{1/2} \} . \end{aligned} \quad (2.10)$$

If the denominator  $Y_{11}Y_{22} - Y_{12}^2 = 0$ , one should interchange the role of  $x$  and  $y$ . If  $Y_{11}Y_{22} - Y_{12}^2 = 0$  and  $X_{11}X_{22} - X_{12}^2 = 0$ ,  $x - x_0$  and  $y - y_0$  are complete squares to begin with. Note that  $\text{Im}\gamma_{\pm}$  may differ from zero and that  $\gamma_- = \gamma_+^*$  in this case. We have:

$$x_{\pm} \equiv x - x_0 + \gamma_{\pm}(y - y_0) = \frac{1}{2}X_{\pm}(\beta_1 + \eta_{\pm}\beta_2)^2 \quad (2.11)$$

with

$$X_{\pm} = X_{11} + \gamma_{\pm}Y_{11} \quad (2.12)$$

and

$$\eta_{\pm} = \frac{X_{12} + \gamma_{\pm}Y_{12}}{X_{11} + \gamma_{\pm}Y_{11}} \quad (2.13)$$

In terms of these new quantities:

$$D_2 \equiv \det \left( \frac{\partial(x, y)}{\partial(\beta_1, \beta_2)} \right) = 2\sqrt{X_+X_-x_+x_-} \frac{\eta_+ - \eta_-}{\gamma_+ - \gamma_-} \quad (2.14)$$

There are two cases to consider, depending on whether  $\text{Im}\gamma_{\pm} \neq 0$  or  $\text{Im}\gamma_{\pm} = 0$ .

If  $\text{Im}\gamma_{\pm} \neq 0$ , let  $\gamma_{\pm} \equiv \gamma_1 \pm i\gamma_2$ ,  $X_{\pm} \equiv X_1 \pm iX_2$ ,  $x_{\pm} \equiv x_1 \pm ix_2$  and  $\eta_{\pm} \equiv \eta_1 \pm i\eta_2$ .  $\gamma_1, \gamma_2, X_1, X_2, x_1, x_2, \eta_1$  and  $\eta_2$  are real. We have:

$$D_2 = 2 \frac{\eta_2}{\gamma_2} \sqrt{X_1^2 + X_2^2} \left[ (x - x_0 + \gamma_1(y - y_0))^2 + \gamma_2^2(y - y_0)^2 \right]^{1/2} \quad (2.15)$$

$D_2 \neq 0$  everywhere except at  $(x, y) = (x_0, y_0)$ . The density  $d \sim \frac{1}{\sigma}$  with

$$\sigma \equiv \sqrt{(x - x_0 + \gamma_1(y - y_0))^2 + \gamma_2^2(y - y_0)^2} \quad (2.16)$$

An illustrative example of a  $\text{Im}\gamma_{\pm} \neq 0$  line caustic is:

$$x = x_0 + X \frac{1}{2}(\beta_1^2 - \beta_2^2) \quad , \quad y = y_0 + Y \beta_1 \beta_2 \quad (2.17)$$

for which  $D = 2\sqrt{Y^2(x - x_0)^2 + X^2(y - y_0)^2}$ . We call a  $\text{Im}\gamma_{\pm} \neq 0$  line caustic "isolated" because it is not attached to any surface caustic. Ring caustics associated with the infall of collisionless dark matter onto a galaxy are line caustics of the isolated type. They will be discussed in detail in sections III and IV.

If  $\text{Im}\gamma_{\pm} = 0$ , then  $x_{\pm}$ ,  $X_{\pm}$  and  $\eta_{\pm}$  are real. From Eq. (2.11) and Eq. (2.14) we see that  $D$  has simple zeros along two surfaces,  $x_+ = 0$  and  $x_- = 0$ , and a double zero on the line where these two surfaces meet. Thus the  $\text{Im}\gamma_{\pm} = 0$  line caustic is "attached" to two generic surface caustics. The following is an illustrative example:

$$x = x_0 + \frac{1}{2}X\beta_1^2, \quad y = y_0 + \frac{1}{2}Y\beta_2^2 \quad (2.18)$$

In this case  $D = 2\sqrt{XY(x - x_0)(y - y_0)}$ , and hence the density  $d \sim \frac{\theta(x-x_0)\theta(y-y_0)}{\sqrt{(x-x_0)(y-y_0)}}$  for  $X, Y > 0$ . We have no use for the "attached" type of line caustic in this paper.



### III. CAUSTIC RINGS

In this section we give a general discussion of the caustic rings that are associated with the infall of collisionless dark matter onto a galaxy. No symmetry is assumed. We do assume that the velocity dispersion of the dark matter particles is small compared to the rotation velocity of the galaxy. We set the velocity dispersion equal to zero and derive the existence of caustics. A small velocity dispersion provides a cutoff, so that the density at the caustic does not become infinite but merely very large.

Fig. 3 shows successive time frames of a set of collisionless particles falling through a galaxy. The particles move purely under the effect of gravity. In Figure 3a, the particles are at first 'turnaround', i.e. they are about to fall onto the galaxy for the first time in their history. They are located on a closed 2D surface surrounding the galaxy in physical space, called the "turnaround sphere". Fig. 3 shows the intersection of this sphere with the plane of the figure, as it evolves in time. For the sake of definiteness it is assumed that the particles carry net angular momentum about the vertical axis. Qualitatively speaking, the turnaround sphere is spinning about the vertical. The particles near the top (bottom) of the sphere in frame a carry little angular momentum and end up near the bottom (top) of the sphere in frame f after falling through the galaxy. The particles near the equator carry the most angular momentum. They form a ring whose radius decreases in time down to some minimum value, reached near frame d, and then increases again. Generally the radius of the sphere at second turnaround is smaller than at first turnaround because the galaxy has grown by infall in the meantime. After second turnaround the sphere falls back in and repeats the same qualitative sequence till third turnaround, and so on.

There is a generic surface caustic associated with the  $m$ th turnaround where  $m = 2, 3, 4, \dots$ . These caustics are located near where the particles of a given outflow reach their maximum radius before falling back in. To see this, parametrize the flow at a given time  $t$  by  $\vec{x}(\alpha, \beta, t_0; t)$  where  $t_0$  is the time the particle was at last turnaround and  $\alpha, \beta$  – for example, spherical coordinates – tell us where the particle was on the turnaround sphere at that time. We define:  $\vec{x}^0 \equiv \frac{\partial \vec{x}}{\partial t_0}$ ,  $\vec{x}^1 \equiv \frac{\partial \vec{x}}{\partial \alpha}$ ,  $\vec{x}^2 \equiv \frac{\partial \vec{x}}{\partial \beta}$ , and  $\dot{\vec{x}} \equiv \frac{\partial \vec{x}}{\partial t}$ . In terms of these:

$$D = \vec{x}^0 \cdot (\vec{x}^1 \times \vec{x}^2). \quad (3.1)$$

Since the discussion is for a fixed time  $t$ , let us not show the  $t$  dependence explicitly further. Let us assume that  $\vec{x}(\alpha, \beta, t_0)$  is near particles at their  $m$ th turnaround with  $m = 2, 3, 4, \dots$ . The spheres  $\{\vec{x}(\alpha, \beta, t'_0) : \forall \alpha, \beta\}$  with  $t'_0$  considerably larger or considerably smaller than  $t_0$  are inside the sphere  $\{\vec{x}(\alpha, \beta, t_0) : \forall \alpha, \beta\}$ . This implies that for all  $\alpha, \beta$  there is a  $t_0(\alpha, \beta)$  such that  $\vec{x}^0(\alpha, \beta, t_0(\alpha, \beta))$  is parallel to the sphere  $\{\vec{x}(\alpha', \beta', t_0(\alpha, \beta)) : \forall \alpha', \beta'\}$ , and hence where  $D = 0$ . Therefore the sphere  $\{\vec{x}(\alpha, \beta, t_0(\alpha, \beta)) : \forall \alpha, \beta\}$  is the location of a generic surface caustic. These *outer* caustics were mentioned in the introduction as the boundaries between the regions with  $n$  flows and those with  $n + 2$  flows where  $n = 1, 3, 5, \dots$ . We do not discuss them further in this paper. Our focus is upon the *inner* caustics which, as we will soon see, have the shape of rings (closed tubes) and which are located near where the particles with the most angular momentum in a given inflow reach their distance of closest approach to the galactic center before moving back out of the galaxy.

To see inner caustic rings, let us return to the sphere of Fig. 3. During each infall-outfall sequence, the sphere turns itself inside out. Indeed, a particle which is part of the flow

and is just inside the sphere in frame b of Fig. 3 is outside the sphere in frame e, and vice-versa. There is therefore a ring of points in space-time which are inside the sphere last. The intersection of this space-time ring with the plane of the figure is at two space-time points, one located at the cusp in frame d, the other at the cusp in frame e. Since there is a continuous flow of spheres falling in and out, the ring just defined is a persistent feature in space. We now show that it is the location of a caustic.

Fig. 4 shows the infall sphere in a neighborhood of space and time where it is completing the process of turning itself inside out. We choose Cartesian coordinates such that  $\hat{y}$  is parallel to the ring at that point;  $\hat{x}$  and  $\hat{z}$  are as shown. We parametrize the flow in a small neighborhood of the ring by  $\vec{\alpha} = (\alpha, \beta, t_0)$  such that  $\frac{\partial x}{\partial \beta} = \frac{\partial z}{\partial \beta} = 0$ . As before,  $t_0$  labels successive infall spheres and may be taken to be the time of their last turnaround. Thus:

$$D = \frac{\partial y}{\partial \beta} \left( \frac{\partial x}{\partial \alpha} \frac{\partial z}{\partial t_0} - \frac{\partial x}{\partial t_0} \frac{\partial z}{\partial \alpha} \right). \quad (3.2)$$

Fig. 4a shows an infall sphere just before it reaches the ring. The line is the intersection of the infall sphere with the plane of the figure.  $\alpha$  labels points along the line. We have  $\frac{\partial z}{\partial \alpha} = 0$  at points A and B because the line is parallel to the  $\hat{x}$ -axis at these points. Similarly,  $\frac{\partial x}{\partial \alpha} = 0$  at point C. Fig. 4b shows an infall sphere at the moment it reaches the ring. Points A, B and C in Fig. 4a have moved to point E in Fig. 4b. Hence  $\frac{\partial z}{\partial \alpha} = \frac{\partial x}{\partial \alpha} = 0$  and therefore  $D = 0$  at point E, which is thus the location of a caustic.

In general,  $D$  only has a simple zero at E, which means that E is the location of a *surface* caustic. We show below that the complete inner caustic surface is a closed tube. E is a point on this tube. In the limit where the transverse size  $p$  of the tube goes to zero, both  $\frac{\partial z}{\partial \alpha} = \frac{\partial x}{\partial \alpha} = 0$  and  $\frac{\partial x}{\partial t_0} = \frac{\partial z}{\partial t_0} = 0$  at E.  $D$  then has a double zero at E. In that limit the tube caustic becomes an *isolated* line caustic where the density diverges as  $\frac{1}{\sigma}$ . When  $p$  is finite but small, the density  $d(\sigma) \sim \frac{1}{\sigma}$  for  $\sigma \gg p$  but has a more complicated behaviour for  $\sigma \sim p$ .

Let us show that the inner caustic must have the topology of a tube, starting with the case of Fig. 3 and generalizing from there. In Fig. 3b,  $\vec{x}^0$  (not shown explicitly) is everywhere pointing outward of the infall sphere because later infall spheres are outside this one. In Fig. 3f,  $\vec{x}^0$  is pointing inside because later infall spheres are inside this one. This implies that during the infall  $\vec{x}^0$  either vanishes at some space-time points or becomes parallel to the sphere. Since  $D = 0$  at such points, they are the location of caustics. Since  $D$  is a continuous function of  $\vec{\alpha}$ , the caustic must lie on a closed surface. Now, if we follow the motion of points which are near the top (bottom) of the sphere in Fig. 3b and end up near the bottom (top) in Fig. 3e,  $\vec{x}^0$  always points up (down).  $\vec{x}^0$  does not vanish and is not parallel to the sphere at any time between these two frames for these points. This implies that there are no inner caustics within some cylinder extending from top to bottom in the spatial volume under consideration in Fig. 3. On the other hand, for the points near the equator in Fig. 3,  $\vec{x}^0$  is pointing outward during infall and is pointing inward during outfall. Thus if we track a point near the equator, at some time  $\vec{x}^0$  either vanishes or is parallel to the sphere. The points where this happens lie on a closed surface which is outside the previously defined cylinder but wraps around it. That surface must therefore be a tube. The tube is located near the equator, where the particles with the most angular momentum are at their distance of closest approach.

Consider now the most general angular momentum distribution on the turnaround

sphere. The angular momentum is a continuous two-dimensional vector field on the sphere. It is well-known that such a vector field must have (at least) two zeros. If we track the particles in the neighborhood of these angular momentum zeros, we find that their  $\vec{x}^0$  does not vanish and is not parallel to the sphere at any time during the infall-outfall sequence. Therefore the inner caustic appears only in the flow of particles which are some distance away from both zeros. Since that set of particles has the topology of a closed ribbon, and the previously defined caustic ring (the set of points E which are in the turnaround sphere last) goes around this closed ribbon once, the inner caustic must be a closed surface with one handle, i.e. a closed tube. Note that the closed tube may self-intersect and may have a complicated shape. However, if the angular momentum is dominated by a smooth component which carries net angular momentum, as was assumed in Fig. 3, then the tube resembles a circle. If there is no angular momentum at all, the tube reduces to a point at the galactic center. As was mentioned in the Introduction, the galactic center is a point caustic in that case, where the density behaves as  $d(r) \sim \frac{1}{r^2}$ .

Fig. 5 shows simultaneous (same  $t$ ) infall spheres near the caustic corresponding to five different initial times:  $t_{01} > t_{02} > \dots > t_{05}$ . The five numbered dots show the positions  $\vec{x}(\alpha, t_{0k}), k = 1 \dots 5$ , for some fixed  $\alpha$  and the five different initial times. Following the dots gives one a qualitative picture of the flow in time. The  $t_{01}$  sphere is falling in but has not yet crossed itself, as in frame b of Fig. 3. The  $t_{02}$  sphere has crossed itself but has not yet completed the process of turning itself inside out, as in frame c of Fig. 3. The  $t_{03}$  sphere is just completing the process of turning itself inside out, as in frame d of Fig. 3. The cusp at point E is the location of a caustic for the reason given earlier. Let  $\alpha_E$  be the value of  $\alpha$  at E. Thus  $\vec{x}(\alpha_E, t_{03})$  is the position of E. In the example of the figure, the particles at the cusp are moving to the left. Thus at  $(\alpha_E, t_{03})$ ,  $\vec{x}$  is pointing to the left whereas  $\vec{x}^0$  is pointing to the right of the  $t_{03}$  infall sphere. For smaller initial times, such as  $t_{05}$ ,  $\vec{x}^0$  is pointing to the left of the infall sphere. Let  $t_{04}$  be the initial time and F be the point where  $\vec{x}^0(\alpha_E, t_0)$  crosses the  $t_0$  sphere. In view of Eq. (3.1), F is the location of a caustic as well. Consider any point which is far from both E and F. At such a point there are two flows because the sphere passes such a point twice, once on the way in and once on the way out. Consider also a point located between E and F. At such a point there are four flows because the sphere passes by four times: at fixed  $t$ , twice for initial time  $t_0$  between  $t_{02}$  and  $t_{03}$ , once between  $t_{03}$  and  $t_{04}$  and once between  $t_{04}$  and  $t_{05}$ . There is therefore a finite compact region in the plane of Fig. 5 inside of which there are four flows and outside of which there are two flows. The boundary of this region, shown as a closed dashed line with three cusps, is the location of the tube caustic. The reason for the three cusps will be given in the next section.

In the limit where the tube shrinks to a line,  $D$  has a double zero on the line. Indeed E and F coincide in that limit.  $\vec{x}^0$  is parallel to the ring at E because  $\vec{x}^0$  is parallel to the infall sphere at F which coincides with E and the infall sphere has a cusp at E. Eq. (3.2) shows that  $D$  has a double zero then which means that the ring is a line caustic. It is of the isolated type since it is not attached to any surface caustics.

In the example of the figure, the initial time  $t_{03}$  of E is after the initial time  $t_{04}$  of F. The opposite is equally possible. Indeed the time reverse of the sequence of Fig. 5 is also a possible sequence and it has the times of E and of F in the opposite order. On the other hand, the density is invariant under time reversal of the flow. This shows that point F is always closer to the galactic center than point E. Note also that if the flow is time reversal

invariant (i.e. if the outfall sequence is the time reverse of the infall sequence), the tube caustic collapses to a line caustic because  $t_{04} = t_{03}$  and hence E and F coincide.

If the successive spheres all fall in exactly the same way, the caustic ring is stationary. In general, however, the trajectories of successive spheres change with time  $t$ , albeit slowly. As a result the caustic ring moves about. However, whether or not it moves, the caustic ring is perfectly sharp in the limit of zero velocity dispersion.

#### IV. THE AXIALLY SYMMETRIC CASE

We assume in this section that the flow of dark matter in and out of the galaxy is axially symmetric about  $\hat{z}$  and symmetric under reflection  $z \rightarrow -z$ . We also assume that the transverse dimensions, called  $p$  and  $q$  below, of the ring caustic are small compared to the ring radius  $a$ . As before, we assume that the dark matter particles are collisionless and we neglect their velocity dispersion. We use the following parametrization of the flow. Let  $R(t_0)$  be the turnaround radius in the  $z = 0$  plane at time  $t_0$ . Then let  $\vec{x}(\theta_0, \varphi_0, t_0; t)$  be the position at time  $t$  of the particle that was at the location of polar coordinates  $(\theta_0, \varphi_0)$  on the sphere of radius  $R(t_0)$  at time  $t_0$ . The density is given by Eqs. (2.2-3) with  $\vec{\alpha} = (\theta_0, \varphi_0, t_0)$  and  $n = 2(4)$  outside (inside) the closed tube caustic described in a general fashion in the previous section.

However, since we assume axial symmetry the motion is in effect two-dimensional. Let  $\rho(\alpha, t_0; t)$  and  $z(\alpha, t_0; t)$  be the cylindrical coordinates at time  $t$  of the ring of particles which start with azimuthal angle  $\theta_0 = \frac{\pi}{2} - \alpha$  at initial time  $t_0$ . One readily shows, repeating for the axially symmetric case the steps which led to Eqs. (2.2-3), that the density is given by:

$$d(\rho, z, t) = \frac{1}{2\pi\rho} \sum_{j=1}^n \frac{d^2 N}{d\alpha dt_0}(\alpha, t_0) \left. \frac{1}{|D_2(\alpha, t_0)|} \right|_{(\alpha, t_0) = (\alpha, t_0)_j} \quad (4.1)$$

where

$$D_2(\alpha, t_0) \equiv \det \left( \frac{\partial(\rho, z)}{\partial(\alpha, t_0)} \right) \quad (4.2)$$

and  $(\alpha, t_0)_j$ , with  $j = 1 \dots n$ , are the solutions of  $\rho = \rho(\alpha, t_0; t)$ ,  $z = z(\alpha, t_0; t)$ . Under a reparametrization of the flow  $(\alpha, t_0) \rightarrow [\alpha'(\alpha, t_0), t'_0(\alpha, t_0)]$ , the determinant transforms according to:

$$D_2(\alpha, t_0) = D'_2(\alpha', t'_0) \det \left( \frac{\partial(\alpha', t'_0)}{\partial(\alpha, t_0)} \right). \quad (4.3)$$

In particular,

$$D_2(\alpha, t_0) = D'_2(\alpha', t'_0) \quad (4.4)$$

for an  $\alpha$ -dependent time shift:  $\alpha' = \alpha$ ,  $t'_0 = t_0 + \Delta t_0(\alpha)$ .

### A. Flow at the caustic

General characteristics of the flow near the caustic are described in section III. Figure 5 constitutes a summary. In the reflection symmetric case, points E and F have  $z = 0$  and  $\alpha = 0$ . Let us reparametrize the flow  $\alpha \rightarrow \alpha$ ,  $t_0 \rightarrow \tau = t_0 + \Delta t_0(\alpha)$  such that  $z(\alpha, \tau = 0) = 0$  for all  $\alpha$ . We expand  $\rho$  and  $z$  in powers of  $\alpha$  and  $\tau$  keeping terms up to second order only. Since we assume the reflection symmetry:  $z \rightarrow -z$ ,  $\rho \rightarrow \rho$ ,  $\alpha \rightarrow -\alpha$ , and  $\tau \rightarrow \tau$ , we have:

$$z = +b\alpha\tau \quad (4.5)$$

$$\rho = \rho_0 - c\tau + \frac{1}{2}u\tau^2 - \frac{1}{2}s\alpha^2, \quad (4.6)$$

where  $b, \rho_0, c, u$  and  $s$  are constants.  $\rho_0$  is the  $\rho$ -coordinate of point E. We may rewrite Eq. (4.6) as

$$\rho = a + \frac{1}{2}u(\tau - \tau_0)^2 - \frac{1}{2}s\alpha^2, \quad (4.7)$$

where  $\tau_0 = c/u$  and  $a = \rho_0 - \frac{1}{2}\frac{c^2}{u}$ .  $a$  is the  $\rho$ -coordinate of point F. The parameters  $b, u$  and  $s$  are positive.  $b$  is positive because the flow is from top to bottom (bottom to top) for particles with  $\alpha > 0$  ( $\alpha < 0$ ).  $u$  is positive because the particles with  $\alpha = 0$  are accelerated outward by the angular momentum barrier.  $s$  is positive because at  $\tau = 0$ , the particles with  $\alpha \neq 0$  are at  $\rho < \rho_0$ .  $\tau_0$  can either be positive or negative.  $a$  is always smaller than  $\rho_0$ , i.e. point F is always closer to the galactic center than point E, as noted earlier.

The determinant is

$$D_2(\alpha, \tau) = -b[u\tau(\tau - \tau_0) + s\alpha^2]. \quad (4.8)$$

It vanishes for

$$\alpha = \pm\sqrt{\frac{u}{s}\tau(\tau_0 - \tau)} \quad (4.9)$$

with  $0 < \tau < \tau_0$  if  $\tau_0 > 0$ , and  $-\tau_0 < \tau < 0$  if  $\tau_0 < 0$ . Substituting Eq. (4.9) into Eqs. (4.5) and (4.7), we find a parametric ( $\tau =$  parameter) representation of the surface of the tube caustic:

$$\begin{aligned} \rho &= a + \frac{1}{2}u(\tau - \tau_0)(2\tau - \tau_0) \\ z &= \pm b\sqrt{\frac{u}{s}\tau^3(\tau_0 - \tau)}. \end{aligned} \quad (4.10)$$

Fig. 6 shows a cross-section of the tube. Its dimensions in the  $\hat{\rho}$  and  $\hat{z}$  directions are  $p = \frac{1}{2}u\tau_0^2$  and  $q = \frac{\sqrt{27}}{4}\frac{b}{\sqrt{us}}p$  respectively. The caustic has three cusps. It is shown below that the appearance of the three cusps is not special to the assumed axial and reflection symmetries nor to the fact that we expanded only to second order in Eqs. (4.5) and (4.6).

First let us note that the caustic has a  $Z_3$  symmetry after an appropriate rescaling. Define the rescaled parameters:

$$T = \frac{\tau}{\tau_0}, \quad A = \sqrt{\frac{s}{u}} \frac{1}{\tau_0} \alpha, \quad (4.11)$$

and the rescaled and shifted (in the  $\hat{\rho}$  direction) coordinates:

$$Z = \frac{2}{b} \sqrt{\frac{s}{u}} \frac{1}{\tau_0^2} z, \quad X = \frac{2}{u\tau_0^2} (\rho - a) - \frac{1}{4}. \quad (4.12)$$

In terms of these, Eqs. (4.5) and (4.7) become:

$$Z = 2AT, \quad X = (T - 1)^2 - A^2 - \frac{1}{4}. \quad (4.13)$$

These relations are invariant under the discrete transformation:

$$\begin{aligned} Z' &= -\frac{1}{2}Z + \frac{\sqrt{3}}{2}X, & X' &= -\frac{\sqrt{3}}{2}Z - \frac{1}{2}X \\ T' &= -\frac{1}{2}T + \frac{\sqrt{3}}{2}A + 3/4, & A' &= -\frac{\sqrt{3}}{2}T - \frac{1}{2}A + \sqrt{3}/4, \end{aligned} \quad (4.14)$$

whose cube is the identity. In the X-Z plane, the transformation is a rotation by  $120^\circ$ . It transforms the 3 cusps of the caustic into one another. Hereafter, let us call the shape of Fig. 6 a “tricusp”. In the language of Catastrophe Theory [6], the tricusp is a  $D_{-4}$  catastrophe.

The apparent reason for the two cusps which are not on the  $\hat{\rho}$ -axis in Fig. 6 is that  $\frac{d\rho}{d\tau}$  and  $\frac{dz}{d\tau}$  both vanish for  $\tau = \frac{3}{4}\tau_0$ . It might be thought that the simultaneous vanishing of  $\frac{d\rho}{d\tau}$  and  $\frac{dz}{d\tau}$  is an accident peculiar to our assumptions of symmetry and/or our limiting the expansion of  $\rho$  and  $z$  to terms of second order in  $\alpha$  and  $\tau$ . But this is not the case. Indeed, consider the equation for the location of a generic caustic in 2 dimensions:

$$D_2(\alpha, \tau) = \frac{\partial \rho}{\partial \alpha} \frac{\partial z}{\partial \tau} - \frac{\partial \rho}{\partial \tau} \frac{\partial z}{\partial \alpha} = 0. \quad (4.15)$$

It defines  $\alpha(\tau)$  such that  $[\rho(\tau) = \rho(\alpha(\tau), \tau), z(\tau) = z(\alpha(\tau), \tau)]$  is a parametric representation of the caustic location. Wherever  $\rho(\tau)$  has an extremum,  $z(\tau)$  may be expected to have an extremum as well since

$$\frac{d\rho}{d\tau} = \frac{\partial \rho}{\partial \alpha} \frac{d\alpha}{d\tau} + \frac{\partial \rho}{\partial \tau} = 0 \quad (4.16)$$

and Eq. (4.15) imply:

$$\frac{dz}{d\tau} = \frac{\partial z}{\partial \alpha} \frac{d\alpha}{d\tau} + \frac{\partial z}{\partial \tau} = 0 \quad (4.17)$$

if  $\frac{d\alpha}{d\tau}$  is finite. The cusp at point E may appear to have a different origin. Its apparent reason is that  $z \sim \pm\tau^{\frac{3}{2}}$  near  $\tau = 0$  which is at the boundary of the range of  $\tau$ . However, this circumstance is an artifact of the parametrization used. Indeed, we saw that the three cusps are transformed into one another by a  $Z_3$  symmetry. As a corollary, the cusp on the  $\hat{\rho}$ -axis can be given the same parametrization as the other two. In conclusion, the appearance of

three cusps in the cross-section of a ring caustic is not an accidental consequence of our simplifying assumptions. Without those assumptions, the cross-section does not have the exact shape of Fig. 6 but it still has three cusps, at least for small deviations from the description given above.

Inside (outside) the tricusp, there are four (two) flows. For example, if we restrict ourselves to the  $z = 0$  plane, then  $\alpha = 0$  or  $\tau = 0$ . If  $\alpha = 0$ , then  $\rho = a + \frac{1}{2}u(\tau - \tau_0)^2 > a$ . If  $\tau = 0$ , then  $\rho = a + \frac{1}{2}u\tau_0^2 - \frac{1}{2}s\alpha^2 < \rho_0$ . Thus for  $z = 0$  and  $\rho > a$ , there are 2 flows:

$$\alpha = 0 \quad , \quad \tau = \tau_0 \pm \sqrt{\frac{2}{u}(\rho - a)} \quad , \quad (4.18)$$

for which

$$\frac{\partial z}{\partial \tau} = 0 \quad , \quad \frac{\partial \rho}{\partial \tau} = \pm \sqrt{2u(\rho - a)} \quad . \quad (4.19)$$

We may call these the “in and out” flows. For  $z = 0$  and  $\rho < \rho_0$ , there are 2 other flows:

$$\tau = 0 \quad , \quad \alpha = \pm \sqrt{\frac{2}{s}(\rho_0 - \rho)} \quad , \quad (4.20)$$

for which

$$\frac{\partial z}{\partial \tau} = \pm b \sqrt{\frac{2}{s}(\rho_0 - \rho)} \quad , \quad \frac{\partial \rho}{\partial \tau} = -u\tau_0 \quad . \quad (4.21)$$

We may call these the “up and down” flows. Therefore, in the  $z = 0$  plane, there are four flows (in, out, up and down) for  $a < \rho < \rho_0$ , whereas there are two flows (up and down) for  $\rho < a$ , and two flows (in and out) for  $\rho > \rho_0$ .

Away from the cusps, the caustic is a generic surface caustic, as described in section IIA. Thus, if one approaches the boundary of the tricusp from the inside and away from any of the cusps, the density increases as  $d \sim \frac{1}{\sqrt{\sigma}}$  where  $\sigma$  is the distance to the boundary. If the boundary is approached from the outside, away from any of the cusps, then the density remains finite until the boundary is reached. For example, for  $z = 0$  and  $\rho - a \rightarrow 0_+$ ,  $D_2 \simeq \mp b\tau_0 \sqrt{2u(\rho - a)}$  for the in and out flows, and hence the density associated with these flows increases as  $\frac{1}{\sqrt{\rho - a}}$ .

Near the cusps, the behaviour depends upon the direction of approach. For  $z = 0$  and  $\rho - \rho_0 \rightarrow 0_-$ ,  $D_2 \simeq -2b(\rho_0 - \rho)$  for the up and down flows and hence  $d \sim \frac{1}{\rho_0 - \rho}$ . For  $z = 0$  and  $\rho - \rho_0 \rightarrow 0_+$ , the density remains finite. For  $\rho = \rho_0$  and  $z \rightarrow 0_{\pm}$ ,  $|D_2| \simeq 3 \left( \frac{u^2 b \tau_0^2 s |z|^2}{2} \right)^{1/3}$  for one of the flows and hence  $d \sim \frac{1}{|z|^{2/3}}$ .

The tube caustic collapses to a line caustic in the limit  $\tau_0 \rightarrow 0$  with  $\frac{b}{\sqrt{us}}$  fixed. In this limit,  $p, q = 0$ ,

$$D_2 = -b(u\tau^2 + s\alpha^2) = -2\sqrt{b^2(\rho - a)^2 + usz^2} \quad , \quad (4.22)$$

and hence the density

$$d(\rho, z) = \frac{1}{2\pi\rho} \frac{d^2N}{d\alpha dt_0} \frac{1}{\sqrt{b^2(\rho - a)^2 + usz^2}} . \quad (4.23)$$

When  $p$  and  $q$  are finite but much smaller than  $a$ , Eq. (4.23) is approximately valid for  $p, q \ll \sigma \ll a$  since the terms of order  $\tau_0$  in Eqs. (4.5), (4.7) and (4.8) are small in this regime.

### B. Relations between the caustic ring parameters and the initial velocity distribution of the dark matter particles

We saw in section IVA that the flow near the caustic is parametrized by the quantities  $b$ ,  $a$ ,  $u$ ,  $s$  and  $\tau_0$ . In this section we relate these quantities to the velocity distribution of the dark matter particles near  $\alpha = 0$  at the initial time  $t_0$ . We assume that the gravitational potential of the galaxy is spherically symmetric, so that the angular momentum of each particle is conserved. As before, we assume  $p, q \ll a$ . Thus the particles participating in the flow at the caustic have  $|\alpha| \ll 1$ . Also the time scale over which the particles cross the caustic is short in that limit, which implies that their velocity is nearly constant while they do so.

As before,  $R(t_0)$  is the turnaround radius of the particles in the equatorial plane ( $\alpha = 0$ ) at time  $t_0$ . Thus the radial velocity of the particles at  $\alpha = 0$ ,  $t = t_0$ , and  $r = R(t_0)$ , vanishes. Consider the velocity distribution of the particles on the sphere of radius  $R(t_0)$  at time  $t_0$  near  $\alpha = 0$ :

$$\begin{aligned} \vec{v}(\theta_0, \varphi_0, t_0) &\equiv \hat{\varphi}_0 v_{\parallel}(\alpha) + \hat{r}_0 v_r(\alpha) - \hat{\theta}_0 v_{\perp}(\alpha) \\ &= \hat{\varphi}_0 [v_{\parallel}(0) + \frac{1}{2} v_{\parallel}''(0) \alpha^2 + 0(\alpha^4)] + \hat{r}_0 [\frac{1}{2} v_r''(0) \alpha^2 + 0(\alpha^4)] \\ &\quad + \hat{\theta}_0 [-\alpha v'_{\perp}(0) + 0(\alpha^3)] , \end{aligned} \quad (4.24)$$

assuming axial and reflection symmetry.  $\hat{r}_0$ ,  $\hat{\varphi}_0$  and  $\hat{\theta}_0$  are the unit vectors in spherical coordinates at location  $(\theta_0, \varphi_0)$  on the sphere. The dependence of  $v_{\parallel}(\alpha)$ ,  $v_{\perp}(\alpha)$  and  $v_r(\alpha)$  upon  $t_0$  is not shown explicitly but is understood. By definition  $v'_{\perp}(0) = \frac{dv_{\perp}}{d\alpha}(0)$ ,  $v''_{\parallel}(0) = \frac{d^2 v_{\parallel}}{d\alpha^2}(0)$ , and so on. We need only discuss the motion of the particles initially at  $\varphi_0 = \frac{\pi}{2}$  since the motion of particles with differing values of  $\varphi_0$  are trivially related by axial symmetry. The particle which is initially at  $\varphi_0 = \frac{\pi}{2}$ ,  $\theta_0 = \frac{\pi}{2} - \alpha$  has angular momentum:

$$\vec{\ell}(\alpha) = R \hat{r}_0 \times \vec{v}(\frac{\pi}{2} - \alpha, \frac{\pi}{2}, t_0) \equiv \ell(\alpha) \hat{\ell}(\alpha) \quad (4.25)$$

where  $R \equiv R(t_0)$  and

$$\ell(\alpha) = R \sqrt{v_{\parallel}^2(\alpha) + v_{\perp}^2(\alpha)} , \quad (4.26)$$

and

$$\hat{\ell}(\alpha) = \cos\phi(\alpha)(\cos\alpha \hat{z} - \sin\alpha \hat{y}) + \sin\phi(\alpha) \hat{x} , \quad (4.27)$$

with



$$\phi(\alpha) = \tan^{-1} \left( \frac{v_{\perp}(\alpha)}{v_{\parallel}(\alpha)} \right) . \quad (4.28)$$

Let  $(x', y')$  be Cartesian coordinates in the plane of the orbit of that particle, with origin at the galactic center. The  $(x', y', z')$  coordinates are related to the  $(x, y, z)$  coordinates by a rotation of angle  $\alpha$  about the  $\hat{x}$ -axis followed by a rotation of angle  $\phi(\alpha)$  about the  $\hat{y}'$ -axis:

$$\begin{pmatrix} x' \\ y' \\ z' \end{pmatrix} = \begin{pmatrix} \cos\phi(\alpha) & \sin\alpha \sin\phi(\alpha) & -\cos\alpha \sin\phi(\alpha) \\ 0 & \cos\alpha & \sin\alpha \\ \sin\phi(\alpha) & -\sin\alpha \cos\phi(\alpha) & \cos\alpha \cos\phi(\alpha) \end{pmatrix} \begin{pmatrix} x \\ y \\ z \end{pmatrix} . \quad (4.29)$$

In the  $(x', y')$  coordinates, the particle starts at  $\vec{r}_0 = R\hat{y}'$  with initial velocity  $\vec{v}_0(\alpha) = -\frac{\ell(\alpha)}{R}\hat{x}' + v_r(\alpha)\hat{y}'$ . See Fig. 7. At the moment of its closest approach to the galactic center, the particle moves with approximately constant velocity:

$$\begin{aligned} x'(\alpha, t_0; t) &= -r_m \cos\delta + V (t - t_m) \sin\delta \\ y'(\alpha, t_0; t) &= -r_m \sin\delta - V (t - t_m) \cos\delta \\ z'(\alpha, t_0; t) &= 0 , \end{aligned} \quad (4.30)$$

where  $r_m$  and  $t_m$  are the distance and time of closest approach,  $V$  is the magnitude of velocity then, and  $\delta$  is defined in Fig. 7. The quantities  $r_m$ ,  $t_m$ ,  $V$  and  $\delta$  depend on  $\alpha$  and  $t_0$ . On the time scale over which the particles cross the ring caustic, the flow is very nearly time-independent, i.e.  $\vec{x}(\alpha, t_0; t) = \vec{x}(\alpha, t - t_0)$ . Hence, we replace  $t - t_m$  by  $t_{0,m} - t_0$  in Eqs. (4.30) where  $t_{0,m}(\alpha)$  is the initial time of the particles which are at their closest approach at time  $t$ . The flow at fixed  $t$  is then given as a function of  $\alpha$  and  $t_0$  by:

$$\begin{aligned} x'(\alpha, t_0) &= -r_m(\alpha) \cos\delta(\alpha) + V(\alpha) \sin\delta(\alpha) (t_{0,m}(\alpha) - t_0) \\ y'(\alpha, t_0) &= -r_m(\alpha) \sin\delta(\alpha) - V(\alpha) \cos\delta(\alpha) (t_{0,m}(\alpha) - t_0) \\ z'(\alpha, t_0) &= 0 . \end{aligned} \quad (4.31)$$

In Eqs. (4.31) and henceforth, the  $t$ -dependence of  $x', y', r_m, \delta, V$  and  $t_{0,m}$  is not explicitly shown.

Using Eqs. (4.29) and (4.31), we have:

$$\begin{aligned} z(\alpha, t_0) &= r_m(\alpha) [\cos\alpha \sin\phi(\alpha) \cos\delta(\alpha) - \sin\alpha \sin\delta(\alpha)] \\ &\quad + V(\alpha) (t_0 - t_{0,m}(\alpha)) [\cos\alpha \sin\phi(\alpha) \sin\delta(\alpha) + \sin\alpha \cos\delta(\alpha)] . \end{aligned} \quad (4.32)$$

As in section IVA, we reparametrize the flow  $t_0 \rightarrow \tau \equiv t_0 - \tau_0(\alpha)$  such that  $z(\alpha, \tau) = 0$  at  $\tau = 0$  for all  $\alpha$ . Thus:

$$z(\alpha, \tau) = V(\alpha) \tau [\cos\alpha \sin\phi(\alpha) \sin\delta(\alpha) + \sin\alpha \cos\delta(\alpha)] . \quad (4.33)$$

The time shift  $\tau_0(\alpha)$  is given by:

$$\begin{aligned} V(\alpha) (\tau_0(\alpha) - t_{0,m}(\alpha)) [\cos\alpha \sin\phi(\alpha) \sin\delta(\alpha) + \sin\alpha \cos\delta(\alpha)] \\ + r_m(\alpha) [\cos\alpha \sin\phi(\alpha) \cos\delta(\alpha) - \sin\alpha \sin\delta(\alpha)] = 0 . \end{aligned} \quad (4.34)$$

Combining Eqs. (4.29), (4.31) and (4.34), we have:

$$\begin{aligned}
x(\alpha, \tau) &= -\cos\phi \sin\delta V\tau - r_m \cos\phi \left[ \cos\delta - \sin\delta \frac{\cos\alpha \sin\phi \cos\delta - \sin\alpha \sin\delta}{\cos\alpha \sin\phi \sin\delta + \sin\alpha \cos\delta} \right] \\
y(\alpha, \tau) &= -V\tau(\sin\alpha \sin\phi \sin\delta - \cos\alpha \cos\delta) \\
&\quad - r_m \left[ \sin\alpha \sin\phi \cos\delta + \cos\alpha \sin\delta \right. \\
&\quad \left. - (\sin\alpha \sin\phi \sin\delta - \cos\alpha \cos\delta) \frac{\cos\alpha \sin\phi \cos\delta - \sin\alpha \sin\delta}{\cos\alpha \sin\phi \sin\delta + \sin\alpha \cos\delta} \right] \quad (4.35)
\end{aligned}$$

with  $V = V(\alpha)$ ,  $\phi = \phi(\alpha)$ ,  $r_m = r_m(\alpha)$  and  $\delta = \delta(\alpha)$ .

We now compare Eqs. (4.33) and (4.35) with Eqs. (4.5) and (4.7) to extract  $b$ ,  $a$ ,  $u$ ,  $\tau_0$  and  $s$ .  $\phi(\alpha)$  is an odd function of  $\alpha$  whereas  $r_m(\alpha)$ ,  $V(\alpha)$  and  $\delta(\alpha)$  are even. Thus:

$$\phi(\alpha) = \phi'(0)\alpha + \frac{1}{6} \phi'''(0)\alpha^3 + 0(\alpha^5) , \quad (4.36)$$

$$r_m(\alpha) = r_m(0) + \frac{1}{2} r_m''(0)\alpha^2 + 0(\alpha^4) , \quad (4.37)$$

and so on. Comparing Eqs. (4.5) and (4.33), we have

$$b = V(0)(\cos\delta(0) + \phi'(0)\sin\delta(0)) . \quad (4.38)$$

We may rewrite Eqs. (4.35) as

$$\begin{aligned}
x(\alpha, \tau) &= x_0(\alpha) + x_1(\alpha)\tau \\
y(\alpha, \tau) &= y_0(\alpha) + y_1(\alpha)\tau , \quad (4.39)
\end{aligned}$$

with the appropriate definitions of  $x_0(\alpha)$ ,  $x_1(\alpha)$ ,  $y_0(\alpha)$ , and  $y_1(\alpha)$ . Therefore

$$\begin{aligned}
\rho(\alpha, \tau)^2 &= x(\alpha, \tau)^2 + y(\alpha, \tau)^2 \\
&= x_0(\alpha)^2 + y_0(\alpha)^2 + 2(x_0(\alpha)x_1(\alpha) + y_0(\alpha)y_1(\alpha))\tau + (x_1(\alpha)^2 + y_1(\alpha)^2)\tau^2 , \quad (4.40)
\end{aligned}$$

which is to be compared with the square of Eq. (4.7):

$$\rho(\alpha, \tau)^2 = a^2 + ua(\tau - \tau_0)^2 - sa\alpha^2 + 0(\tau^3, \tau_0^3, \alpha^2\tau) . \quad (4.41)$$

For  $\alpha = 0$  this yields:

$$\begin{aligned}
a^2 + ua\tau_0^2 &= x_0^2(0) + y_0^2(0) \\
-ua\tau_0 &= x_0(0) x_1(0) + y_0(0) y_1(0) \\
ua &= x_1^2(0) + y_1^2(0) . \quad (4.42)
\end{aligned}$$

From Eqs. (4.35) and (4.39), we have:

$$\begin{aligned}
x_0(0) &= -r_m(0) \left[ \cos\delta(0) - \sin\delta(0) \frac{\phi'(0) \cos\delta(0) - \sin\delta(0)}{\phi'(0) \sin\delta(0) + \cos\delta(0)} \right] \\
x_1(0) &= -V(0) \sin\delta(0) \\
y_0(0) &= -r_m(0) \left[ \sin\delta(0) + \cos\delta(0) \frac{\phi'(0) \cos\delta(0) - \sin\delta(0)}{\phi'(0) \sin\delta(0) + \cos\delta(0)} \right] \\
y_1(0) &= V(0) \cos\delta(0) .
\end{aligned} \tag{4.43}$$

Hence:

$$\begin{aligned}
a &= r_m(0) \\
u &= \frac{V(0)^2}{r_m(0)} \\
\tau_0 &= \frac{r_m(0)}{V(0)} \frac{\phi'(0) \cos\delta(0) - \sin\delta(0)}{\phi'(0) \sin\delta(0) + \cos\delta(0)} .
\end{aligned} \tag{4.44}$$

Comparing Eqs. (4.40) and (4.41) for  $\alpha \neq 0$ , we have:

$$-sa = (x_0(0)x_0''(0) + y_0(0)y_0''(0)) . \tag{4.45}$$

A somewhat lengthy calculation yields:

$$\begin{aligned}
s &= - \frac{r_m''(0)(1 + \phi'(0)^2)}{[\phi'(0)\sin\delta(0) + \cos\delta(0)]^2} \\
&\quad - r_m(0) \frac{\phi'(0)\cos\delta(0) - \sin\delta(0)}{[\phi'(0)\sin\delta(0) + \cos\delta(0)]^3} \left\{ -\frac{2}{3} \phi'(0) \right. \\
&\quad \left. + \frac{1}{3} (\phi'''(0) - \phi'(0)^3) - (1 + \phi'(0)^2) \delta''(0) \right\} .
\end{aligned} \tag{4.46}$$

Our derivation of the caustic parameters assumes that  $p$  and  $q = \frac{\sqrt{27}}{4} \frac{b}{\sqrt{us}} p$  are much smaller than  $a$ . Using Eqs. (4.44), we have:

$$p = \frac{1}{2}a \left( \frac{\phi'(0)\cos\delta(0) - \sin\delta(0)}{\phi'(0)\sin\delta(0) + \cos\delta(0)} \right)^2 . \tag{4.47}$$

Thus the treatment requires that  $\phi'(0)$  and  $\delta(0)$ , or at least the combination  $\phi'(0)\cos\delta(0) - \sin\delta(0)$ , be small compared to one.

Eqs. (4.38), (4.44) and (4.46) express the caustic parameters in terms of the values of  $\phi(\alpha)$ ,  $r_m(\alpha)$ ,  $V(\alpha)$  and  $\delta(\alpha)$  and their first few derivatives at  $\alpha = 0$ .  $\phi(\alpha)$  is given in terms of the initial velocity distribution by Eq. (4.28). Moreover, angular momentum conservation implies:

$$r_m(\alpha) = \frac{\ell(\alpha)}{V(\alpha)} \tag{4.48}$$

with  $\ell(\alpha)$  given by Eq. (4.26). Thus, to achieve our goal of determining the caustic parameters in terms of the initial velocity distribution, it remains to express  $V(\alpha)$  and  $\delta(\alpha)$  in terms of  $v_r(\alpha)$ ,  $v_{\parallel}(\alpha)$  and  $v_{\perp}(\alpha)$ .

This last step can only be carried out if we adopt a model for the galactic gravitational potential  $U(r, t)$  in which the particles fall. To illustrate the process, let us adopt the time-independent potential:

$$U(r) = v_{rot}^2 \ln\left(\frac{R}{r}\right) \quad (4.49)$$

which yields (perfectly) flat rotation curves with rotation velocity  $v_{rot}$ . Since particle energy is conserved for this potential, we have:

$$V(\alpha) = \left[ 2v_{rot}^2 \ln\left(\frac{R}{a}\right) + v_r^2(\alpha) + v_{\parallel}^2(\alpha) + v_{\perp}^2(\alpha) \right]^{\frac{1}{2}}. \quad (4.50)$$

The angle  $\delta = \delta(\ell, v_r)$  was determined numerically for the potential  $U(r)$  by solving the equations of motion of a particle falling from the initial position  $\vec{r}_0 = R\hat{y}'$  with initial velocity  $\vec{v}_0 = \frac{-\ell}{R}\hat{x}' + v_r\hat{y}'$ ; see Fig. 7. Table I gives  $\delta$  as a function of  $j = \frac{\ell}{Rv_{rot}}$  and  $\nu = \frac{v_r}{v_{rot}}$ .

A simple velocity distribution is that corresponding to an initially rigidly rotating turnaround sphere:  $v_{\perp}(\alpha) = 0$ ,  $v_r(\alpha) = 0$  and  $v_{\parallel}(\alpha) = v_{\parallel}(0)\cos\alpha$ . Let us explore what happens in this case. Since  $\phi(\alpha) = 0$ , we have:

$$\begin{aligned} p &= \frac{1}{2}a \tan^2\delta(0) \\ q &= \frac{\sqrt{27}}{4} p \frac{\cos^2\delta(0)}{\sqrt{-\frac{r_m''(0)}{r_m(0)} - \tan\delta(0)\delta''(0)}}. \end{aligned} \quad (4.51)$$

Typical values in fits of the infall model [11,8,9] to observed properties of our galaxy are  $j \sim 0.25$  and  $a \sim \frac{jR}{\sqrt{2\ln(R/a)}} \sim 0.1R$ . Table I shows that  $\delta$  is slowly varying and of order 0.5 then. For  $\phi'(0) = 0$ , this implies  $p \sim 0.15 a$ . For small  $j$ ,  $V \simeq v_{rot}\sqrt{2\ln(R/a)}$  is approximately  $\alpha$ -independent. For the above special velocity distribution, we have then  $r_m(\alpha) = r_m(0)\cos\alpha$  and hence  $q \simeq \frac{\sqrt{27}}{4} p \cos^2\delta(0) \sim p$ .

### C. Flow some distance away from the caustic

In this section, we give a qualitative description of the flow associated with a caustic ring on distance scales of order  $a$ , the ring radius. To this effect, we choose the special initial velocity distribution corresponding to an initially rigidly rotating turnaround sphere:  $v_r(\alpha) = v_{\perp}(\alpha) = 0$ ,  $v_{\parallel}(\alpha) = v_{\parallel}(0)\cos\alpha$ . Also we neglect the  $\alpha$ -dependence of  $V$  and set  $\delta = 0$ . Table I shows that the latter approximation is valid only for  $j \ll 1$ , i.e.  $a \ll R$ . We also take the velocity  $\vec{V}$  of each particle to be constant while it travels distances of order  $a$ . These crude approximations yield a description of the flow which is topologically correct and which can be derived by simple analytical methods, but which is likely to agree only qualitatively with actual flows. In particular, since  $\phi(\alpha)$  and  $\delta(\alpha)$  are set equal to zero, the tricusp structure of the caustic is shrunk to a point.

For the assumed velocity distribution,

$$\ell(\alpha) = \ell_{max} \cos\alpha \quad (4.52)$$

with  $\ell_{max} = Rv_{\parallel}(0)$ . Since we neglect the  $\alpha$ -dependence of  $V$ ,

$$r_m(\alpha) = a \cos\alpha \quad (4.53)$$

with  $a = \frac{\ell_{max}}{V}$ . Since we set  $\phi(\alpha) = 0$  and  $\delta(\alpha) = 0$ , Eqs. (4.33) and (4.35) become:

$$\begin{aligned} x(\alpha, \tau) &= -a \cos\alpha \\ y(\alpha, \tau) &= V\tau \cos\alpha \\ z(\alpha, \tau) &= V\tau \sin\alpha . \end{aligned} \quad (4.54)$$

From Eqs. (4.54), one obtains:

$$\rho D_2(\alpha, \tau) = -V \cos\alpha (a^2 \sin^2\alpha + V^2 \tau^2) = -V \cos\alpha \sqrt{(r^2 - a^2)^2 + 4a^2 z^2} . \quad (4.55)$$

Inserting this into Eq. (4.1) and using  $d\Omega = 2\pi \cos\alpha d\alpha$ , we have:

$$d(\rho, z) = \frac{2}{V} \frac{d^2 N}{d\Omega dt_0} \frac{1}{\sqrt{(r^2 - a^2)^2 + 4a^2 z^2}} \quad (4.56)$$

where  $\frac{d^2 N}{d\Omega dt_0}$  is the rate at which the dark matter particles fall in per unit solid angle.

The velocity fields can also be derived. One finds:

$$\begin{aligned} v_z &= -\frac{\partial z}{\partial \tau} = -V \sin\alpha = \mp \frac{V}{a} \sqrt{\frac{1}{2} \left( a^2 - r^2 + \sqrt{(r^2 - a^2)^2 + 4a^2 z^2} \right)} \\ v_\rho &= \frac{-1}{2\rho} \frac{\partial \rho^2}{\partial \tau} = -\frac{V^2 \tau \cos^2\alpha}{\rho} \\ &= \mp \text{sign}(z) \frac{V}{2a^2 \rho} \sqrt{\frac{1}{2} \left( r^2 - a^2 + \sqrt{(r^2 - a^2)^2 + 4a^2 z^2} \right)} \left( r^2 + a^2 - \sqrt{(r^2 - a^2)^2 + 4a^2 z^2} \right) \\ v_\varphi &= +\sqrt{V^2 - v_z^2 - v_\rho^2} , \end{aligned} \quad (4.57)$$

where the  $\mp$  signs are for the down and up flows. In the galactic plane ( $z = 0$ ) we have:

$$\begin{aligned} v_z &= \mp V \sqrt{1 - \frac{r^2}{a^2}} && \text{for } r < a \\ &= 0 && \text{for } r > a \\ v_\rho &= 0 && \text{for } r < a \\ &= \pm V \sqrt{1 - \frac{a^2}{r^2}} && \text{for } r > a \\ v_\varphi &= V \frac{r}{a} && \text{for } r < a \\ &= V \frac{a}{r} && \text{for } r > a . \end{aligned} \quad (4.58)$$

## V. GRAVITATIONAL EFFECTS OF CAUSTICS

The gravitational force per unit mass caused by the particles in a zero-velocity dispersion flow  $\vec{x}(\vec{\alpha}, t)$  is:

$$\begin{aligned}\vec{F}(\vec{x}, t) &= Gm \int d^3x' \frac{d(\vec{x}', t)}{|\vec{x}' - \vec{x}|^3} (\vec{x}' - \vec{x}) \\ &= Gm \int d^3\alpha \frac{d^3N}{d\alpha_1 d\alpha_2 d\alpha_3} (\vec{\alpha}) \frac{\vec{x}(\vec{\alpha}, t) - \vec{x}}{|\vec{x}(\vec{\alpha}, t) - \vec{x}|^3}\end{aligned}\quad (5.1)$$

where  $m$  is the mass of each particle. We are particularly interested in the effect of caustic rings on galactic rotation curves. Since caustic rings migrate only on cosmological time scales [9], which are much longer than gas dynamic time scales, it is reasonable to expect the gas in the galactic plane to have relaxed to orbits consistent with the dark matter distribution in the caustics.

If the gas or other material in the galactic plane at radius  $r$  moves on a circular orbit with velocity  $v(r)$ , then

$$\frac{v^2(r)}{r} = F(r) \quad (5.2)$$

is the inward gravitational force per unit mass at radius  $r$ . Let us assume that a circular ring caustic lies in the galactic plane at radius  $a$ . In the spirit of perturbation theory, let  $v(r) = v_{rot} + v_1(r)$  and  $F(r) = F_0(r) + F_1(r)$ , where  $F_1(r)$  is the inward force per unit mass due to the caustic and  $v_1(r)$  is the perturbation the caustic causes in the rotation curve. If the matter in the caustic were smoothly distributed, the rotation curve would be flat with value  $v_{rot}$ . At zeroth order,  $F_0(r) = \frac{v_{rot}^2}{r}$ . At first order,

$$F_1(r) = \frac{2}{r} v_{rot} v_1(r). \quad (5.3)$$

Let us assume that  $p, q, |r - a| \ll a$  where  $p$  and  $q$  are the transverse dimensions of the caustic ring. In that limit we may, when calculating  $F_1(r)$ , neglect the curvature of the ring and pretend that it is a straight tube. After integrating over the length of the tube, we have

$$F_1(r) \simeq 2Gm \int d\rho \int dz \frac{d(\rho, z)}{(r - \rho)^2 + z^2} (r - \rho). \quad (5.4)$$

Using Eq. (4.1), changing variables  $(\rho, z) \rightarrow (\alpha, t_0)$ , neglecting the  $(\alpha, t_0)$  dependence of  $\frac{dM}{d\Omega dt_0} = \frac{m}{2\pi \cos(\alpha)} \frac{dN}{d\alpha dt_0}$  over the size of the caustic, and approximating  $\rho(\alpha, t_0)$  by  $a$  in the Jacobian factor, we obtain

$$F_1(r) \simeq \frac{2G}{a} \frac{dM}{d\Omega dt_0} \int d\alpha dt_0 \frac{r - \rho(\alpha, t_0)}{(r - \rho(\alpha, t_0))^2 + z^2(\alpha, t_0)}. \quad (5.5)$$

Ref. [9] indicates how to extract the prefactor  $\frac{dM}{d\Omega dt_0}$  from the self-similar infall model. Here we focus on the profile of  $v_1(r)$  implied by the structure of caustic rings. The functions  $\rho(\alpha, t_0)$  and  $z(\alpha, t_0)$  are given by Eqs. (4.5) and (4.7) respectively (replace  $\tau$  by  $t_0$ ). One finds:

$$v_1(r) \simeq \frac{4\pi G}{v_{rot} b} \frac{dM}{d\Omega dt_0} I\left(\zeta, \frac{r-a}{p}\right) \quad (5.6)$$

where  $\zeta = su/b^2$  and

$$I(\zeta, X) \equiv \frac{1}{2\pi} \int dA dT \frac{X - (T-1)^2 + \zeta A^2}{[X - (T-1)^2 + \zeta A^2]^2 + 4A^2 T^2} . \quad (5.7)$$

Fig. 8 shows  $I(\zeta, X)$  as a function of  $X$  for  $\zeta = 1.0$ . For  $X < 0$  ( $r < a$ ) and  $X > 1$  ( $r > a + p$ ),  $I(\zeta, X)$  is constant. For  $0 < X < 1$  (inside the tricusp),  $I(\zeta, X)$  rises by an amount  $\Delta I(\zeta)$ .  $\Delta I = 1$  for  $\zeta = 1$ . Fig. 9 shows  $\Delta I$  as a function of  $\zeta$ . In the limit where the tricusp collapses to a point ( $p \rightarrow 0$ ), there is a discontinuity in  $v_1(r)$  at the caustic ring radius:

$$\Delta v_1 \simeq \frac{4\pi G}{v_{rot} b} \frac{dM}{d\Omega dt_0} \Delta I(\zeta) . \quad (5.8)$$

The profile shown in Fig. 8 should be added to a descending rotation curve so that the total rotation curve, with the effect of the caustic ring included, remains flat on average. Fig. 10 gives a qualitative description.

## VI. CONCLUSIONS

We discussed the appearance of caustics in the flow of collisionless particles with negligible velocity dispersion. Caustics are locations in physical space where the density diverges in the limit of zero velocity dispersion. This happens wherever the 3D sheet on which the particles lie in 6D phase-space folds back. The generic caustic is a surface at the boundary between two regions in physical space, one of which has  $n$  flows and the other  $n+2$  flows. The density diverges as  $\frac{1}{\sqrt{\sigma}}$ , where  $\sigma$  is the distance to the surface, on the side with  $n+2$  flows. We discussed line caustics as well. These are a degenerate case where the density diverges as  $1/\sigma$  where  $\sigma$  is the distance to the line. We divided line caustics into two types: "attached" ( $Im\gamma_{\pm} = 0$ ) and "isolated" ( $Im\gamma_{\pm} \neq 0$ ). In the latter the density is finite everywhere except on the line, whereas in the former the line is at the intersection of two surface caustics.

We discussed the fall of collisionless dark matter with negligible velocity dispersion in and out of a galaxy. Two types of caustic form: outer caustics which are spherical surfaces surrounding the galaxy and inner caustics which are rings. The caustic rings are located near where the particles with the most angular momentum are at their closest approach to the galactic center. The surface of the ring is a closed tube whose cross-section is a closed line which has three cusps one of which points away from the galactic center. The tube is the location of a generic surface caustic. Inside the tube there are four flows whereas outside there are two flows. In the limit where the transverse dimensions of the tube vanish the ring is a closed line caustic of the isolated variety.

We analyzed the ring caustic in detail in the case of axial symmetry about the  $\hat{z}$ -axis, of reflection symmetry  $z \rightarrow -z$ , and where the transverse dimensions,  $p$  and  $q$ , of the tube are much smaller than the ring radius  $a$ . The caustic is then described by 5 parameters:  $a$ ,  $u$ ,  $s$ ,  $t_0$  and  $b$ . The precise shape of a transverse section of the ring in this limit is shown in Fig. 6. The 5 parameters were determined in terms of the initial velocity distribution of the infalling dark matter particles assuming the gravitational potential of the galaxy to be

spherically symmetric. Also, a qualitative description was given of the flow of dark matter particles on length scales of order  $a$ .

Finally we discussed the gravitational effects of caustic rings, in particular the perturbation in a galactic rotation curve caused by a ring lying in the galactic plane. Figs. 8, 9 and 10 describe the shape and size of the bump implied by the tricusp structure of the caustic ring.

## VII. ACKNOWLEDGEMENTS

I thank John Klauder for stimulating comments. This work was supported in part by the US Department of Energy under grant DE-FG02-97ER41029 and by a Fellowship from the J. S. Guggenheim Memorial Foundation.



## REFERENCES

- [1] E.W. Kolb and M.S. Turner, *The Early Universe*, Addison-Wesley, 1990; M. Srednicki, Editor *Particle Physics and Cosmology: Dark Matter*, North-Holland, 1990.
- [2] S. Tremaine and J.E. Gunn, Phys. Rev. Lett. **42** 407 (1979); J.R. Bond, G. Efstathiou and J. Silk, Phys. Rev. Lett. **45** 1980 (1980); S.D.M. White, C.S. Frenk and M. Davis, Ap. J. **274** L1 (1983).
- [3] Y.B. Zel'dovich, Astrofizika **6** 319 (1970), Astron. Ap. **5** 84 (1970).
- [4] V. de Lapparent, M.J. Geller and J.P. Huchra, Ap.J. **302** L1 (1986).
- [5] S. Tremaine, astro-ph/9812146.
- [6] R. Gilmore, *Catastrophe Theory for Scientists and Engineers*, Wiley, 1981.
- [7] P. Sikivie and J. Ipser, Phys. Lett. **B291** 288 (1992).
- [8] P. Sikivie, I. Tkachev and Y. Wang, Phys. Rev. **D56** 1863 (1997).
- [9] P. Sikivie, Phys. Lett. **B432** 139 (1998).
- [10] J. A. Filmore and P. Goldreich, Ap. J. **281** 1 (1984); E. Bertschinger, Ap. J. Suppl. **58** 39 (1985).
- [11] P. Sikivie, I. Tkachev and Y. Wang, Phys. Rev. Lett. **75** 2911 (1995).
- [12] C.J. Hogan, astro-ph/9811290.
- [13] A.G. Doroshkevich et al., M.N.R.A.S. **192** 321 (1980); A.A. Klypin and S.F. Shandarin, M.N.R.A.S. **204** 891 (1983); J.M. Centrella and A.L. Melott, Nature **305** 196 (1983); A.L. Melott and S.F. Shandarin, Nature **346** 633 (1990).

## TABLES

TABLE I. Values of  $\delta$  as a function of  $j$  and  $\nu$ .

$\nu \rightarrow$	-0.2	-0.1	0.0	+0.1	+0.2
$j \downarrow$					
0.05	0.28	0.29	0.29	0.30	0.30
0.10	0.34	0.36	0.37	0.38	0.38
0.15	0.38	0.40	0.42	0.43	0.44
0.20	0.41	0.44	0.46	0.48	0.49
0.25	0.43	0.46	0.49	0.52	0.54
0.30	0.45	0.48	0.52	0.55	0.58
0.35	0.46	0.50	0.54	0.58	0.62
0.40	0.46	0.51	0.56	0.61	0.65
0.45	0.46	0.52	0.58	0.63	0.68
0.50	0.46	0.53	0.59	0.66	0.72

## FIGURES

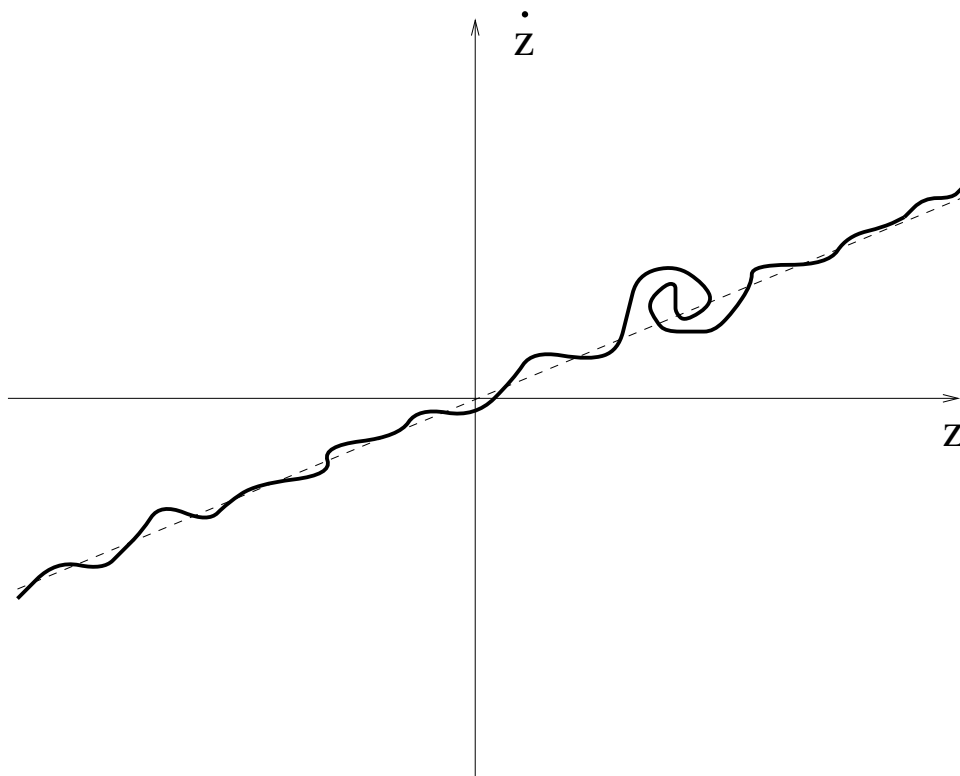


FIG. 1. The wiggly line is the intersection of the  $(z, \dot{z})$  plane with the 3D sheet on which the collisionless dark matter particles lie in phase-space. The thickness of the line is the primordial velocity dispersion. The amplitude of the wiggles in the  $\dot{z}$  direction is the velocity dispersion associated with density perturbations. Where an overdensity grows in the non-linear regime, the line winds up in clockwise fashion. One such overdensity is shown.

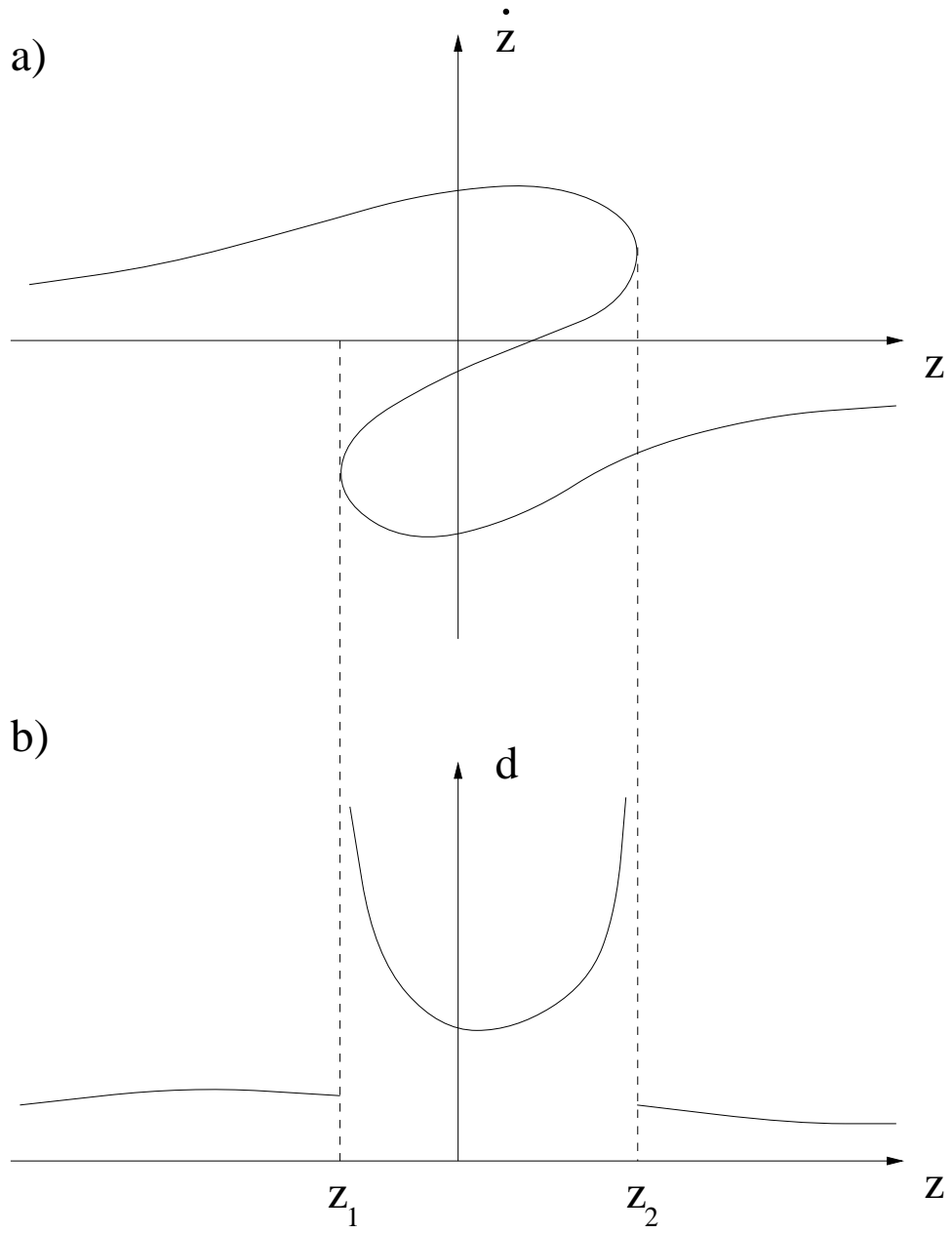


FIG. 2. A generic surface caustic in phase-space (a) and in physical space (b). The two dimensions ( $x$  and  $y$ ) into which the caustic extends as a surface are not shown. The physical space density  $d$  diverges at those locations ( $z_1$  and  $z_2$ ) where the phase-space sheet folds back.

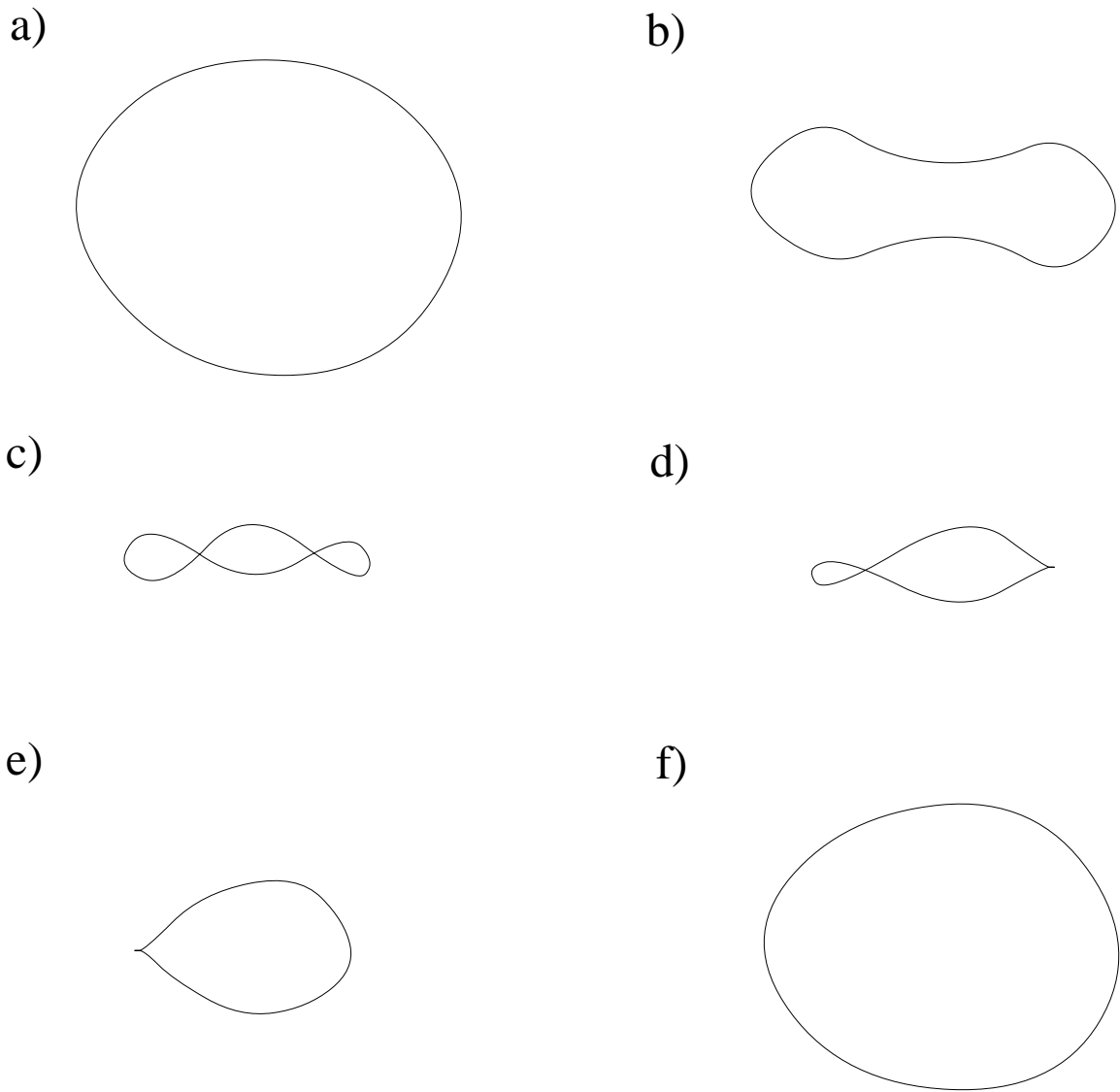


FIG. 3. Infall of a turnaround sphere. The closed lines are at the intersections of the sphere with the plane of the figure at six successive times. The sphere has net angular momentum about the vertical axis. It crosses itself between frames b) and c). After frame e) the sphere has completed the process of turning itself inside out. The cusps in frames d) and e) are at the intersection of a caustic ring with the plane of the figure.

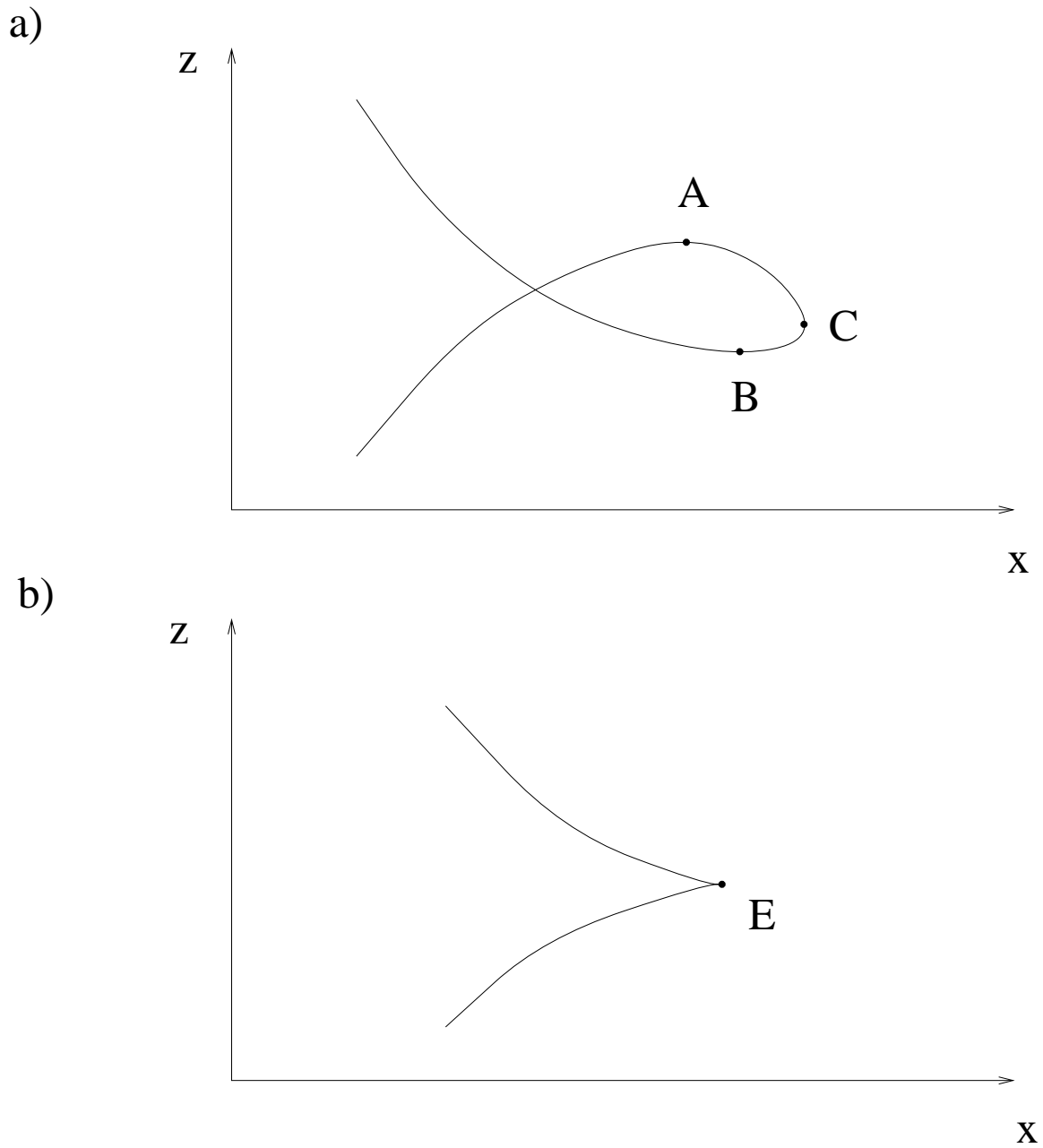


FIG. 4. An infall sphere near where and when it completes the process of turning itself inside out. The lines are at the intersections of the sphere with the plane of the figure at two successive times, corresponding to frames c and d in Fig. 3.  $\alpha$  labels points along the line.  $\frac{\partial z}{\partial \alpha} = 0$  at points A and B.  $\frac{\partial x}{\partial \alpha} = 0$  at point C. Points A, B and C move to point E, which is thus the location of a caustic since  $D = 0$  there.

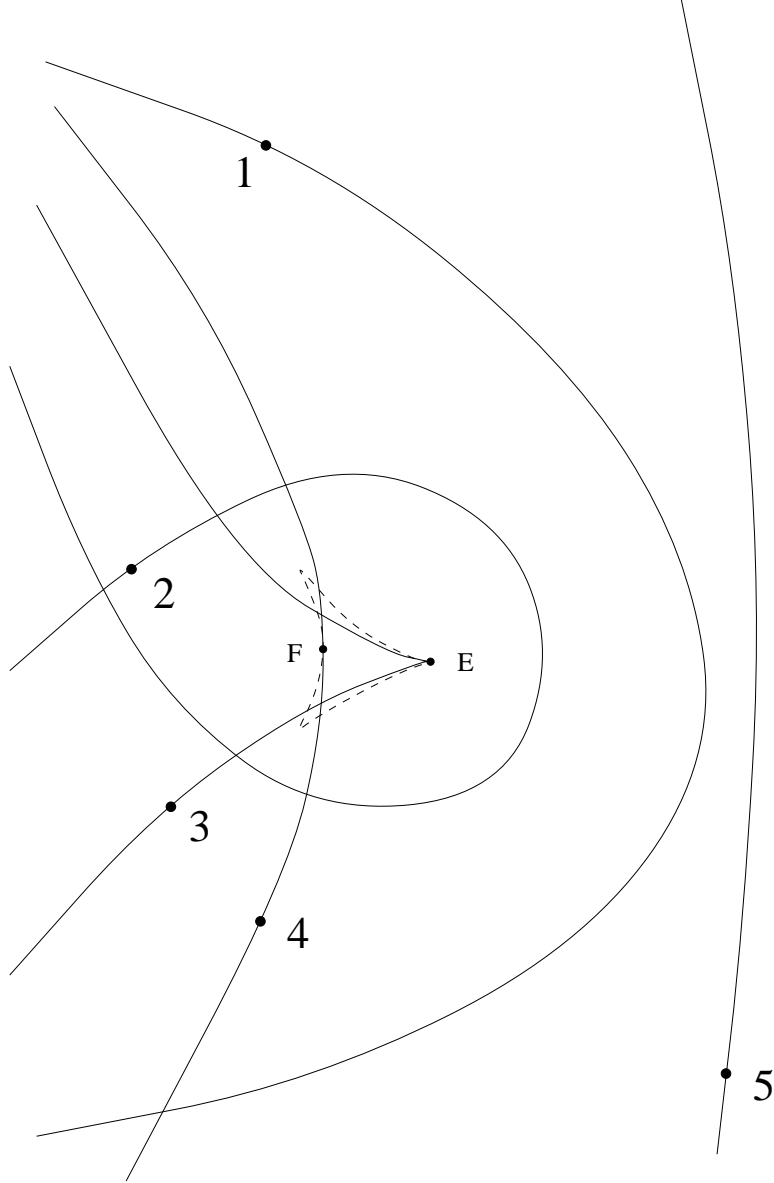


FIG. 5. Qualitative description of the flow near a caustic ring. The solid lines are at the intersection of five simultaneous infall spheres corresponding to different initial times  $t_{05} < t_{04} < \dots < t_{01}$ . The five numbered points are at  $\vec{x}(\alpha, t_{0k}), k = 1 \dots 5$ , for some value of  $\alpha$ . Points E and F are defined in the text. The closed dashed line is at the intersection of the caustic tube with the plane of the figure. There are four flows inside the dashed line whereas outside there are two. The galactic center is to the left of the figure.

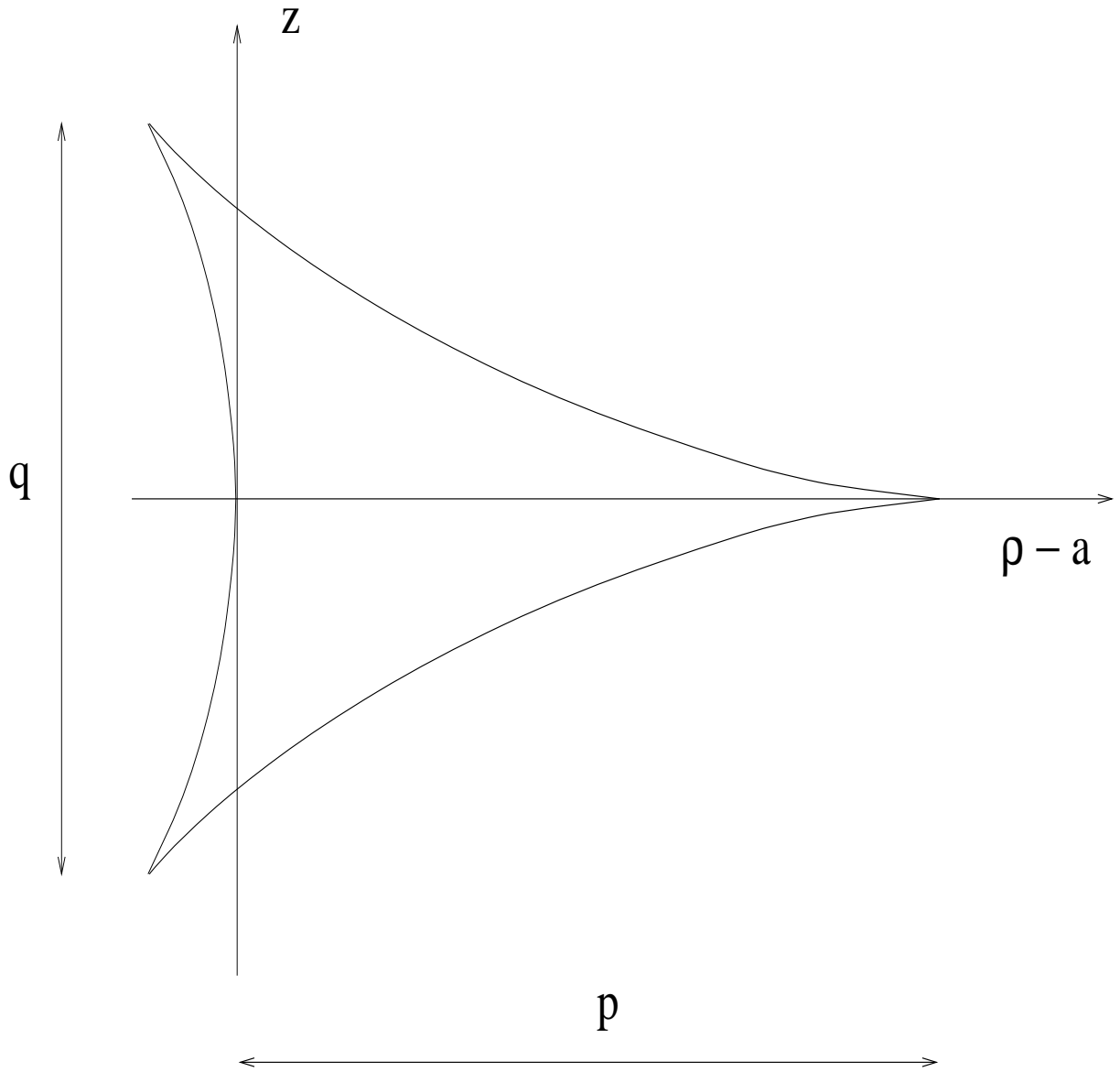


FIG. 6. Cross-section of a caustic ring in the case of axial and reflection symmetry, and  $p, q \ll a$ .



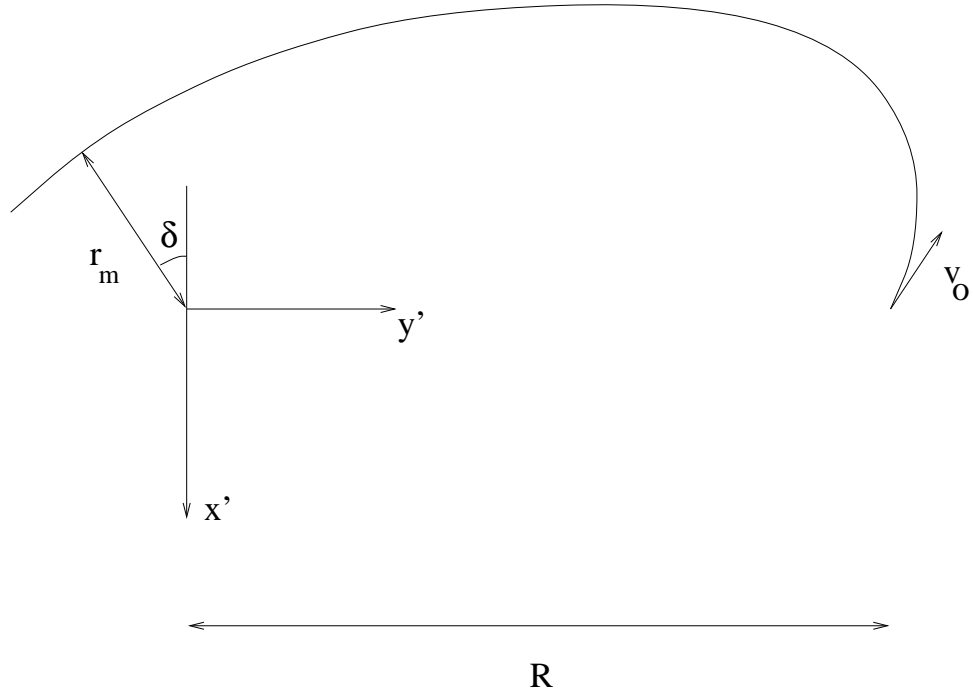


FIG. 7. Trajectory of a dark matter particle falling onto a galaxy.  $\vec{v}_0$  is the velocity at the initial time  $t_0$ .  $r_m$  is the distance of closest approach to the galactic center.

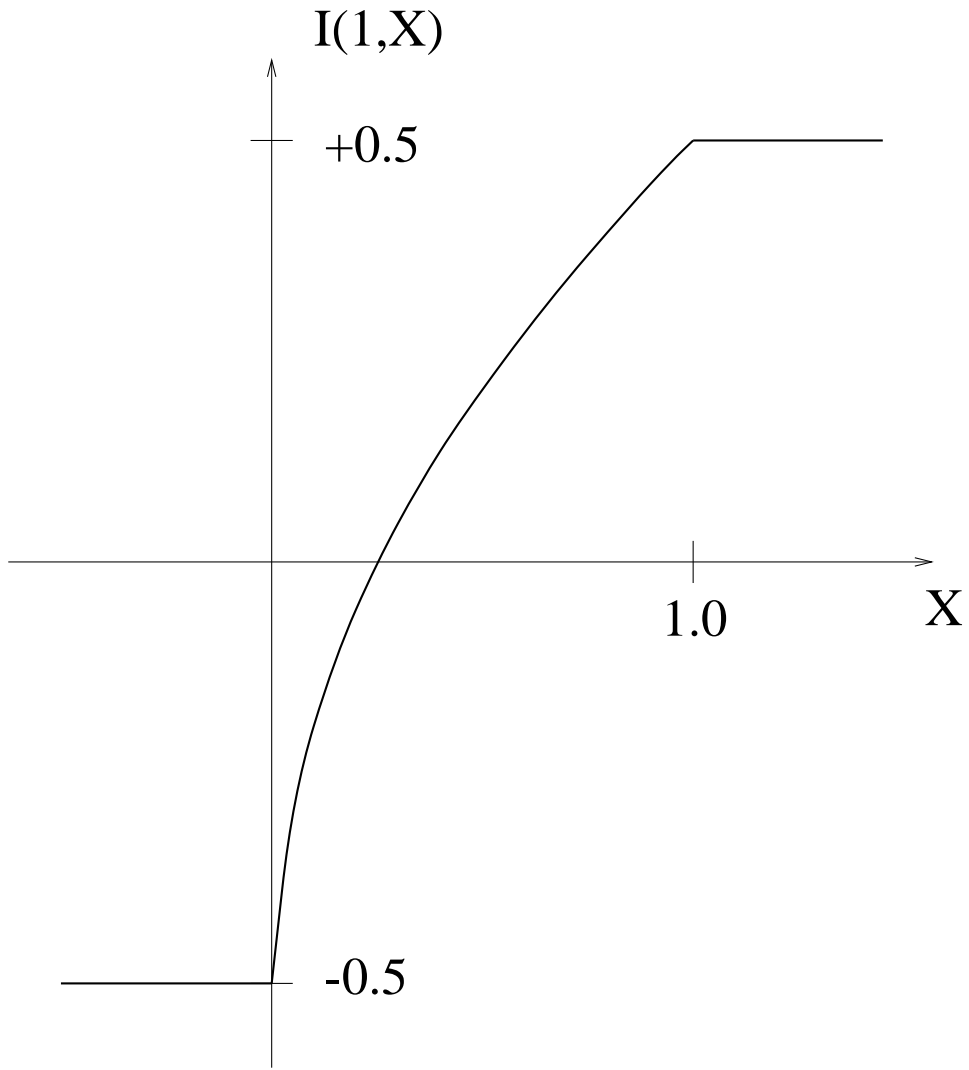


FIG. 8. Plot of the function  $I(\zeta, X)$  for  $\zeta = 1.0$ .

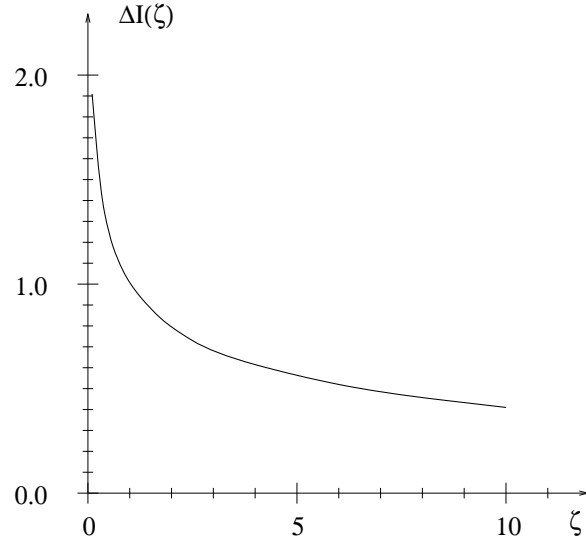


FIG. 9. Plot of the  $\Delta I(\zeta)$  as a function of  $\zeta$ .

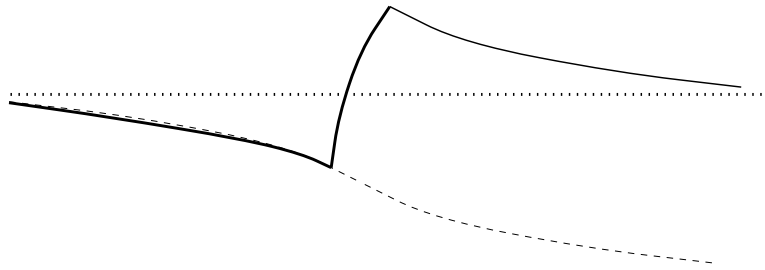


FIG. 10. Qualitative description of the effect of a caustic ring upon a galactic rotation curve if the caustic ring lies in the galactic plane. The horizontal dotted line represents the flat rotation curve if the matter in the caustic ring is smoothly distributed. The descending dashed line is the rotation curve after the matter in the caustic ring has been removed. The solid line is the rotation curve in the presence of the caustic ring. It is the sum of the dashed curve and the profile of Fig. 8.